GEOLOGICA CARPATHICA, OCTOBER 2014, 65, 5, 339–364 doi: 10.2478/geoca-2014-0024

Taphonomic implications from Upper Triassic mass flow deposits: 2-dimensional reconstructions of an ammonoid mass occurrence (Carnian, Taurus Mountains, Turkey)

ALEXANDER LUKENEDER and SUSANNE MAYRHOFER

Natural History Museum, Geological-Palaeontological Department, Burgring 7, A-1010 Wien, Austria;
alexander.lukeneder@nhm-wien.ac.at; susanne.mayrhofer@nhm-wien.ac.at

(Manuscript received January 22, 2014, accepted in revised form October 7, 2014)

Abstract: Ammonoid mass occurrences of Late Triassic age were investigated in sections from Aşağıyaylabel and Yukarıyaylabel, which are located in the Taurus Platform-Units of eastern Turkey. The cephalopod beds are almost monospecific, with >99.9 % of individuals from the ceratitic genus *Kasimlarceltites*, which comprises more than hundreds of millions of ammonoid specimens. The ontogenetic composition of the event fauna varies from bed to bed, suggesting that these redeposited shell-rich sediments had different source areas. The geographical extent of the mass occurrence can be traced over large areas up to 10 km^2. Each of the Early Carnian (Julian 2) ammonoid mass occurrences signifies a single storm (e.g. storm-wave action) or tectonic event (e.g. earthquake) that caused gravity flows and turbidity currents. Three types of ammonoid accumulation deposits are distinguished by their genesis: 1) matrix-supported floatstones, produced by low density debris flows, 2) mixed floatstones and packstones formed by high density debris flows, and 3) densely ammonoid shell-supported packstones which result from turbidity currents. Two-dimensional calculations on the mass occurrences, based on sectioning, reveal aligned ammonoid shells, implying transport in a diluted sediment. The ammonoid shells are predominantely redeposited, preserved as mixed autochthonous/parautochnonous/allochthonous communities based on biogenic and sedimentological concentration mechanisms (= *in-situ* or post-mortem deposited). This taphonomic evaluation of the *Kasimlarceltites* beds thus reveals new insights into the environment of deposition of the Carnian section, namely that it had a proximal position along a carbonate platform edge that was influenced by a nearby shallow water regime. The *Kasimlarceltites*-abundance zone is a marker-zone in the study area, developed during the drowning of a shallow water platform, which can be traceable over long distances.

Key words: *Kasimlarceltites*, ammonoid mass occurrence, taphonomy, Triassic, Taurus Mountains, Turkey.

Introduction

Upper Triassic sediments, especially of the Carnian age, form the major element within the Taurus Mountains. The area around Aşağıyaylabel has already been investigated by Özgül & Arpat (1973), Dumont & Kerey (1975), Monod (1977), Poisson (1977), Gutnic et al. (1979), Robertson (1993, 2000), Şenel (1997), Gindl (2000), Robertson et al. (2003), Lukeneder et al. (2012) and Lukeneder & Lukeneder (2014).

The Carnian section at Aşağıyaylabel displays a lithological change from pure carbonatic to more siliciclastic sedimentation (Lukeneder et al. 2012). The facies change occurs exactly at the Lower–Upper Carnian boundary (=Julian–Tuvalian boundary), and represents the beginning of the so-called Carnian Pluvial Event in the section at Aşağıyaylabel. Facies interpretations change from open platform margin conditions, through deeper shelf margin conditions, to finally open marine-influenced basinal conditions (Lukeneder et al. 2012).

During the Carnian time, the sediments around the area of Aşağıyaylabel were deposited within an intrashelf area on the western end of the Cimmerian System (Gindl 2000; Stampfli & Borel 2002; Lukeneder et al. 2012). Sedimentological and paleontological investigations show a delayed carbonate factory collapse during that time.

Lower Carnian faunal elements, exclusively detected at Aşağıyaylabel and characterized as *Kasimlarceltites krystyni*, *Klipsteinia disciformis* and *Anasirenites crassicrenulatus* (Lukeneder & Lukeneder 2014) indicate a rather isolated but still connective paleoceanographic position of the intrashelf area on the western end of the Cimmerian System.

The present study examines deposits representing an acme zone, registered within the Upper Triassic (Carnian) Kartoz and Kasımlar formations, which crop out at Aşağıyaylabel (=Kartoz) and Yukarıyaylabel (=Karapınar). This acme zone is characterized by several beds yielding ammonoid mass occurrences of the Carnian ammonoid-genus *Kasimlarceltites*. The aim of the present work is to detail the distribution and taphonomy of the *Kasimlarceltites* mass occurrence at the lowermost part of the Kasımlar Formation within the Julian 2. Results on taphonomy and environmental processes, obtained by the two dimensional analyses of sections, thin sections, as well as by conclusions from outcrop logs and block data, are presented. This leads to a more detailed picture of the sedimentological dynamics, hence to a better understanding of the taphonomy and sedimentology of such Upper Triassic shell beds (e.g. ammonoids). Dynamic processes for specific mass flow deposits (e.g. debris flows, grain flows or turbidity currents; Middleton & Hampton 1973, 1976; Flügel 1978, 2004; Lowe 1982; Brown &

Loucks 1993; Stow & Mayall 2000; Mulder & Alexander 2001; Kawakami & Kawamura 2002; Potter et al. 2005; Nichols 2009; SEPM 2014), also termed gravity flows or density currents, will be discussed in respect to resedimentation of sediments and biogenic components. The determination of specific mechanisms in terms of the genesis concerning event bed deposition, storm deposition, shell accumulation and the consequences for the facies and bioclastic fabric were reported and discussed in Aigner (1982a, 1985), Einsele & Seilacher (1982), Kreisa & Bambach (1982), Brett & Baird (1986), Kidwell (1986, 1991a,b, 1993a,b), Kidwell et al. (1986), Tucker & Wright (1990), Brett & Seilacher (1991), Chuanmao et al. (1993), Einsele et al. (1991a,b), Seilacher & Aigner (1991), Soja et al. (1996), Hips (1998), Fürsich & Pandey (1999), Martin (1999), Storms (2001), Lukeneder (2003a,b, 2004a,b), Fernández-López (2007), Montiel-Boehringer et al. (2011), and Pérez-Lopéz & Pérez-Valera (2012).

The result is a detailed succession of abundance or accumulation layers (i.e. distinct layers with ammonoid mass occurrences) within an acme zone in the Upper Triassic of the Aşağıyaylabel section. Such 'ammonoid-beds' are the result of bio-events, which are often manifested by the abundance or mass occurrence of ammonoids (Lukeneder 2001, 2003b). The presented paper is a first step and the initial point for the lateral correlation of such ammonoid mass occurrences and establishment of ammonoid abundance zones within the Taurus Mountains. Trigger mechanisms and potential scenarios, causing the accumulation of such ammonoid shell beds, are discussed.

Geographical setting

The Aşağıyaylabel (AS) sections (i.e. AS I–AS IV) are located in southwest Turkey, about 90 km northeast of Antalya and approximately 70 km southeast of Isparta (Figs. 1–3). Aşağıyaylabel is accessible from the two major cities of the region, Eğirdir and Beyşehir, located 50 km and 40 km away, respectively. The locality adjoins the small village Aşağıyaylabel (1000 m above sea level) on the northern slope of an east-west trending ridge, between 1050 m to 1100 m at N 37°33′05″ and E 31°18′16″. The former

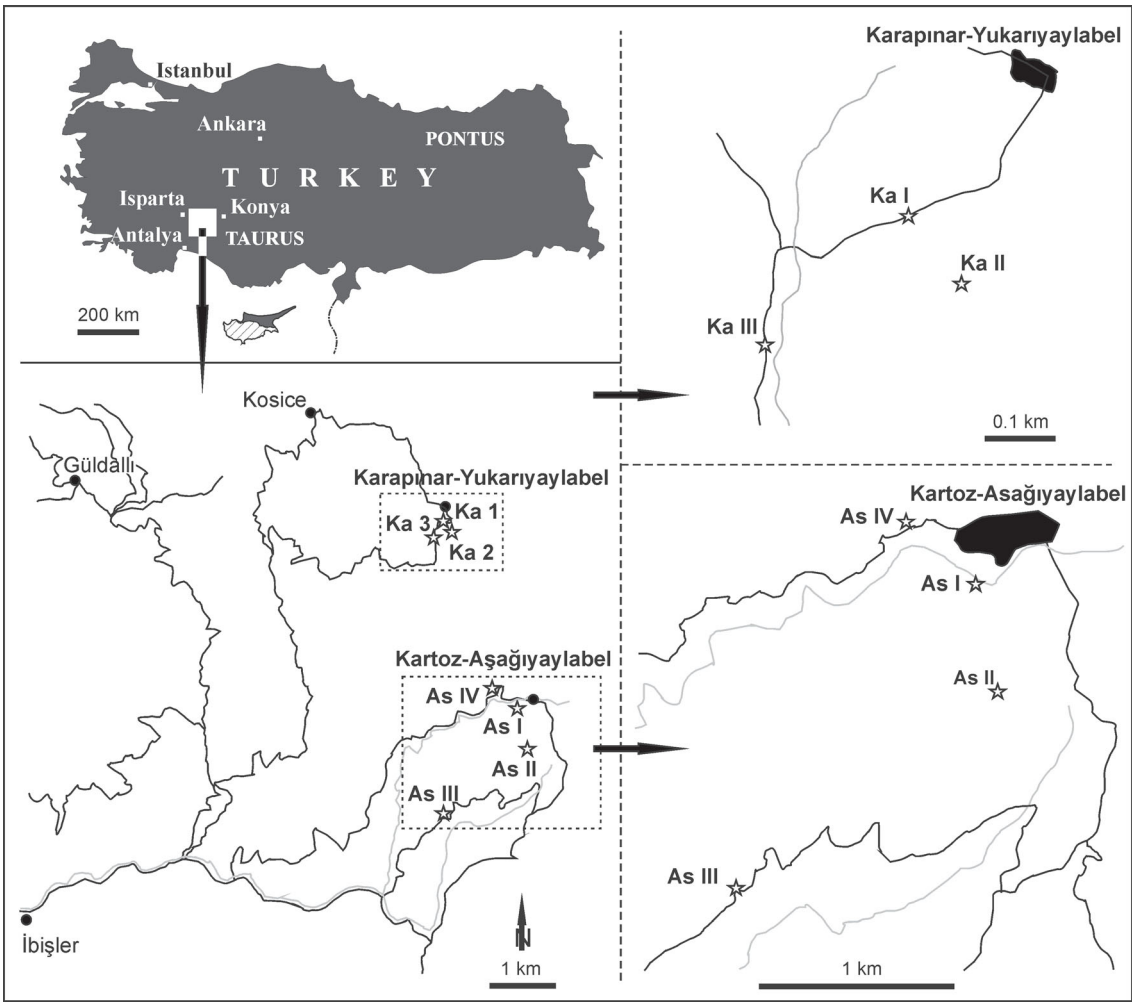

Fig. 1. Locality map of the investigated area showing the outcrops of Upper Triassic sediments around the area of Aşağıyaylabel (=Kartoz) and Yukarıyaylabel (=Karapınar) within the the Anamas Dağ carbonate platform in the Taurus Mountains (southwest Turkey). Investigated sections are indicated as AS I, II, III and IV and KA I, II and III.

name of Aşağıyaylabel was Kartoz, after which the Kartoz Formation was named (Dumont 1976; Gindl 2000; Lukeneder et al. 2012; Lukeneder & Lukeneder 2014).

A particular depositional situation is marked by the small, Triassic (Late Carnian — Julian 2) blocks containing ammonoid mass occurrences, which are included within a Cenozoic conglomerate fan (Deynoux et al. 2005), mainly formed by Triassic sediments from the nearby area at AS III (Figs. 1, 3).

The Yukarıyaylabel (=Karapınar, KA) sections (i.e. KA I–KA III) are located 5 km to the north of the Aşağıyaylabel (AS) sections (Figs. 1, 2, 4) near a small road through the village. The village is situated at 1328 m to 1340 m above sea level with N 37°57′69″ and E 31°29′12″.

Geological setting

Geologically the area is located on the Anamas Dağ carbonate platform or Anamas-Akseki Autochthonous. The Anamas Dağ is part of the so-called Taurus-Platform-Units between the Antalya Suture in the South and the İzmir-Ankara Suture in the North, south of the Isparta Angle (Robertson 1993; Şenel 1997; Andrews & Robertson 2002; Robertson et al. 2003). The Anamas-Akseki Autochthonous (=Karacahisar-Autochthonous) includes Middle to Upper Triassic limestones, marlstones and shales of up to 500 m thickness (Gindl 2000). The geology of southwestern Turkey and the Anamas Dağ carbonate platform has been extensively investigated by Özgül & Arpat (1973), Dumont & Kerey (1975), Monod (1977), Poisson (1977), Gutnic et al. (1979), Robertson (1993, 2000), Şenel (1997), and Robertson et al. (2003).

The deposits of this area belong to two formations, the stratigraphically older Kartoz Formation (earliest Carnian), and the younger Kasımlar Formation (Carbonate, Marlstone and Shale member; Lukeneder et al. 2012), which reaches from Early to Late Carnian age (Julian 2 — Tuvalian 1). The fossil fauna (Lukeneder & Lukeneder 2014) reported within this work derives from the Kasımlar Formation with Lower Carnian to Upper Carnian sediments (Julian 2 — Tuvalian 1; Fig. 2).

The paleogeographic domain of the Anatolian System (Taurus Mts, Turkey) was characterized during Triassic times by microplates located in the middle of the western Tethys Ocean. The investigated succession was deposited in an intra-shelf basin of equatorial paleolatitude at the western end of the 'Cimmerian terranes' or 'Cimmerian blocks' (Şengör et al. 1984; Scotese et al. 1989; Dercourt et al. 1993, 2000; Scotese 1998, 2001; Gindl 2000; Stampfli & Borel 2002; Stampfli et al. 2002; Lukeneder et al. 2012; Lukeneder & Lukeneder 2014). This area was located between the 'old' Paleotethys in the North and the Neotethys in the South during the Late Triassic (Carnian, 228–216 Ma — Gindl 2000; Gradstein et al. 2012). While the Paleotethys Ocean underwent subduction along the southern margin of Eurasia, the young Neotethys Ocean (southern branch of Neotethys, sensu Şengör & Yılmaz 1981) was widened between the African continent and the Cimmerian terranes, which consisted of Turkey, Iran, Afghanistan, Tibet, and Malaysia (Golonka 2004). In the North of these Cimmerian terranes the İzmir-Ankara Ocean (northern branch of the Neotethys, sensu Şengör & Yılmaz 1981) and the 'old' Paleotethys were still open to the East (Tekin et al. 2002; Golonka 2004; Tekin & Göncüoğlu 2007; Göncüoğlu et al. 2010).

Lithology and facies

The Triassic succession of Aşağıyaylabel starts with an angular unconformity above Carboniferous rocks (Dumont 1976; Gindl 2000). The main formations are the Middle to Upper Triassic Kartoz Formation (Late Carnian) and the Kasımlar Formation (uppermost Lower Carnian to Upper Carnian). The Kartoz Formation consists of shallow-water platform carbonates with thick-shelled bivalves (megalodonts) and corals. In contrast, the overlying Kasımlar Formation starts disconformably (i.e. hiatus) with an 8-m-thick pile of deeper-water limestones; this precedes 12 m marlstone-part into shales (Fig. 2). The section is dated based on conodonts, ammonoids, and halobiids (Lukeneder et al. 2012; Lukeneder & Lukeneder 2014). A detailed age assignment follows Krystyn et al. (2002) and Gallet et al. (2007). The strata dip approximmately 50° towards the Northeast.

The studied successions at Aşağıyaylabel (=Kartoz) and Yukarıyaylabel (=Karapınar) start with shallow-water limestones of the Kartoz Formation, with thick-shelled bivalves and corals (Lukeneder et al. 2012; Lukeneder & Lukeneder 2014; Fig. 2). This phase ends with a corroded and iron oxide-stained dissolution surface (without any traces of boring), pointing probably to subaerial exposure or sedimentological omission. The Kartoz Formation represents a drowned carbonate platform and is disconformably overlain by deeper-water, hemipelagic, black limestones of the Kasımlar Formation, which includes, at its base (i.e. 1.8–16.0 m) levels of thin ammonoid floatstone- and packstone layers (*Kasimlarceltites* beds=acme *range* zone — Fig. 2). This lower part is followed by a thick slump breccia (e.g. preserved at AS I and AS IV), containing up to meter-sized patch reef blocks (interpreted as Cipit-boulders by Lukeneder et al. 2012) together with comparably small ammonoid coquinas and filament limestone components. The Lower to Upper Carnian boundary is marked by a change to grey limy marlstones, with rare ammonoid- and pelagic-bivalve-bearing layers, passing upwards into a thick pile of sterile dark shale with thin silty and rare siliciclastic interbeds. Microfacies analyses identify the Carnian depositional system around Aşağıyaylabel and Yukarıyaylabel as an intrashelf platform environment grading upwards into deeper zones, influenced by pelagic conditions (Lukeneder et al. 2012).

All sections where the ammonoid mass occurrence of *Kasimlarceltites* exists start with shallow water carbonates of the Kartoz Formation (Figs. 2, 3). Coral-bafflestones, megalodontid limestones and shallow water breccias predominate. This facies is characterized by a dense abundance of *in-situ* corals and megalodontid shells (Lukeneder et al. 2012), trapped by a cortoid grainstone matrix representing an open platform environment.

Directly above an unconformity, the younger Kasımlar Formation is divided into the Carbonate member (units A, B, and C), the Marlstone member, and the Shale member. The

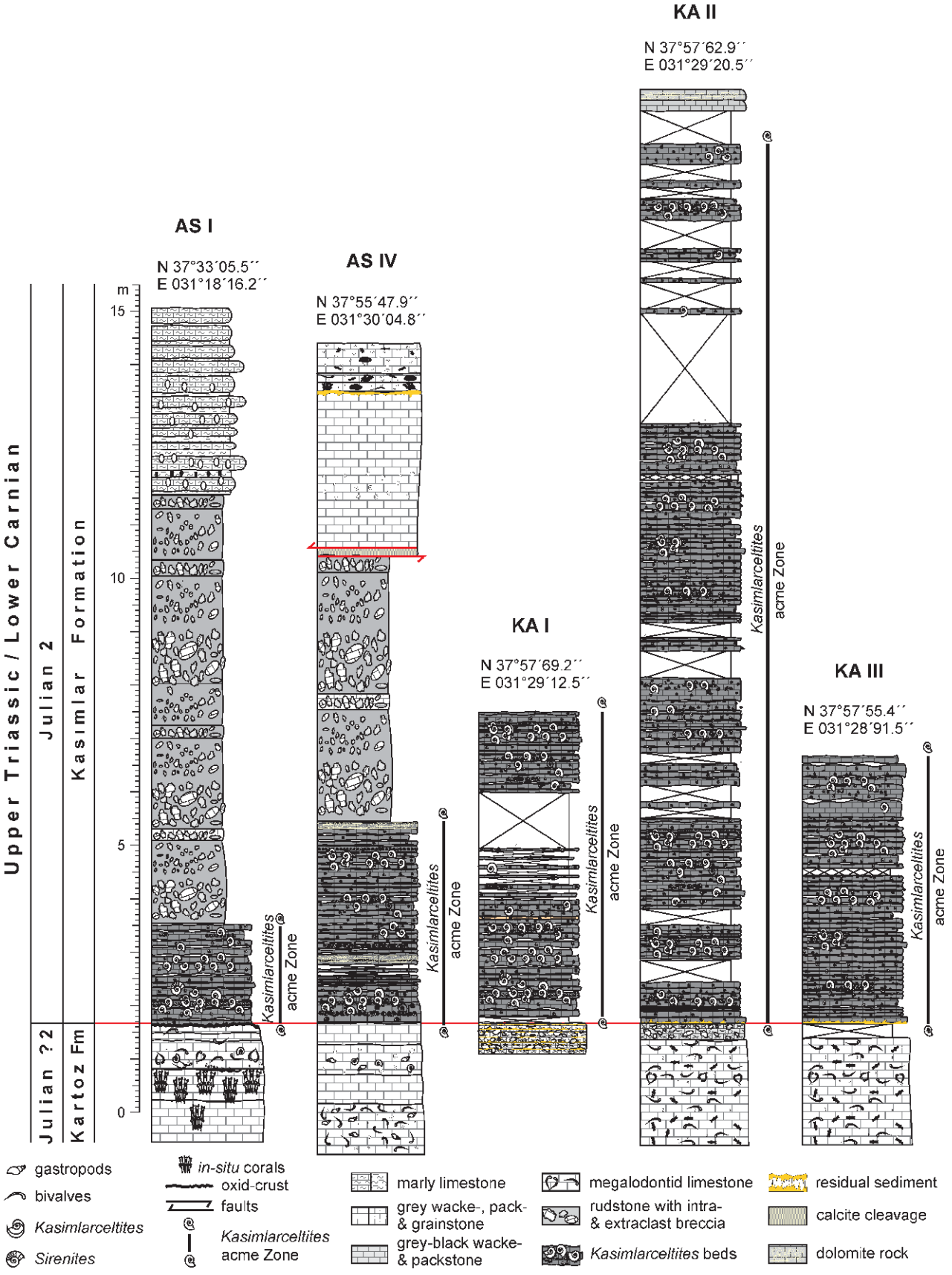

Fig. 2. Lithology and biostratigraphy (left) of the section investigated at Aşağıyaylabel and Yukarıyaylabel with indicated occurrences and ranges of the *Kasilmarceltites* acme zone.

lowermost Carbonate member appears at the base with the *Kasimlarceltites* beds (acme zone). The *Kasimlarceltites* beds are bioclastic pelagic wackestones, which were deposited in a deep shelf margin or mid ramp position (Lukeneder et al. 2012; see Flügel 1978, 2004 for facies types). The faunal spectrum mirrors two different source areas of the bioclastic input: thin-shelled bivalves (halobiids), which are most common, represent the autochthonous component (deeper shelf margin), whereas the original habitat of the benthic foraminifera (lagenids), the thick-shelled bivalves (megalodontiids), and the large, low-spired gastropods was situated on a fore slope or on a shallow marine ramp. Tilted geopetal fills of gastropods and ammonoids (e.g. *Kasimlarceltites*), together with clasts of eroded semilithified sedimentary layers ('plasticlasts'), prove episodic erosion, downward transport, and resedimentation. Bioturbation has mostly obliterated the original arrangement of autochthonous fine grained sediments (together with thin-shelled bivalves and radiolaria) alternating with coarser-grained 'tempestitic' or 'turbidtitic' layers. When the original layering is preserved, bedding planes are strongly affected by stylolites. Common authigenic pyrite (mostly well-developed as cubic crystals) in different levels of the section is probably of synsedimentary origin. As indicated by the high abundance of halobiid bivalves and the dark-coloured sediment, it could point to temporary dysaerobic conditions of the bottom waters and/or the pore-fluids of the unconsolidated sediments (Flügel 1978, 2004; McRoberts 2010).

Material and fossil assemblage

The fossil material was collected by the authors (1995–2011), by Mathias Harzhauser and Franz Topka (both Natural History Museum Vienna), and on earlier field excursions (1980–1997) by Leopold Krystyn, Andreas Gindl and Philip Strauss (excursion organized by the University of Vienna). All specimens described within this study have been extensively collected from the Kasımlar Formation at the sections Aşağıyaylabel and Yukarıyaylabel, which consists of a Lower Carnian (*Austrotrachyceras austriacum* Zone) ammonoid fauna (Lukeneder & Lukeneder 2014). The ammonoid fauna contains ammonoids of all ontogenetic stages.

The ammonoids are well preserved, phragmocones are mostly filled with secondary calcite and the shell is neomorphically replaced by secondary calcite. Due to the fact that draught filling (=draft filling; Seilacher 1968; Maeda & Seilacher 1996; Olivero 2007) is absent, which led to a preserved primary phosphatic siphuncle, a fast deposition and sedimentation after death can be assumed. Only a few specimens of the genera *Kasimlarceltites*, *Klipsteinia*, *Anasirenites* and *Megaphyllites* show suture lines. A total of 479 ammonoid specimens, two nautiloid specimens and four coleoid specimens have been collected (Lukeneder & Lukeneder 2014). The ammonoid assemblages consist of 12 ammonoid genera with *Kasimlarceltites*, *Spirogmoceras*, *Sandlingites*, *Klipsteinia*, *Neoprotrachyceras*, *Sirenites*, *Anasirenites*, *Paratropites*, *Trachysagenites*, *Proarcestes*, *Megaphyllites*, *Joannites*, *Simonyceras,* containing 13 species, a single coleoid genus (*Atractites*), and a single nautiloid species.

The ammonoids are clearly dominated by the genus *Kasimlarceltites* with more than 100 million specimens (counting method: see Mayrhofer & Lukeneder, in prep.), due to the fact that it is the main faunal element of the mass occurrences, followed by *Sirenites* with 56 specimens.

The matrix contains mainly juvenile to adult halobiid bivalves (i.e. *Halobia rugosa*), megalodontid shells, gastropods (i.e. *Omphaloptycha* type), chaetitids, corals, calcareous sponges, sponge spicules, foraminifera, radiolaria, dasycladaceaes, cyanobacteria, peloids, and planktic crinoids (e.g. *Osteocrinus*). Lower Carnian conodonts are present with *Gladigondolella* and *Metapolygnathus*.

Detailed stratigraphic sections of the Lower to Upper Carnian interval were measured and described from Aşağıyaylabel (=Kartoz, AS) and Yukarıyaylabel (=Karapınar, KA). 325 thin-sections of 200 layers, collected in 2007 and 2012, were made and used for petrographic studies. Additional sectioning and polishing was performed on block samples in longitudinal, horizontal and tangential (90°) directions for reconstructions of the orientation and alignment of the ammonoids (see Potter & Pettijohn 1977; Futterer 1982; Olivero 2007) within the mass occurrence. The corresponding bed numbers are indicated by the abbreviation AS (for Aşağıyaylabel) and KA (for Yukarıyaylabel=Karapınar), by the corresponding succession number (as there are several successions at each locality AS I–AS IV resp. KA I–KA III) and the corresponding bed number (e.g. AS I/1=sample from Aşağıyaylabel, succession I, bed 1). Additional facies investigations were conducted under a dissecting microscope (Zeiss Discovery V20) with attached digital camera (AxioCam MRc5). Sectioning and photographing were done at the Natural History Museum in Vienna (NHMV=NHMW).

Detailed petrographic analyses were done using a petrographic polarization microscope from Leica (Leica DDM4500P) and a digital camera (Leica DFC4420). Sectioning and photographing were done at the Natural History Museum Vienna and at the University of Vienna (Department of Petrography).

The material is stored within the collection of the Geological-Paleontological Department of the NHMV. The inventory numbers of blocks are: for AS I NHMW 2012/0133/0551–0561, for NHMW AS II 2014/0094/0001, for AS III NHMW 2014/0095/0001, for AS IV NHMW 2014/0091/0001–0007, for KA I NHMW 2014/0092/0001–0003, for KA II NHMW 2014/0093/0001–0004, and for KA III 2014/0096/0001.

Biostratigraphy

The sections at Aşağıyaylabel (AS I–AS IV) and the biochrono-stratigraphically equivalent sections at Karapınar (KA I–KA IV) comprise about 50 m of essentially calcareous beds passing into marlstones (in part marly limestones) and shaly beds with considerable siliciclastic input at the top. The lowermost part is represented by the Kartoz Formation, an Upper Triassic (earliest Carnian; Fig. 2) light-grey, shallow-water carbonate succession. It comprises corals and thick-shelled bivalves. *Neoprotrachyceras* sp., found in the lower part of bed AS I/2, dates at least the top of the Kartoz

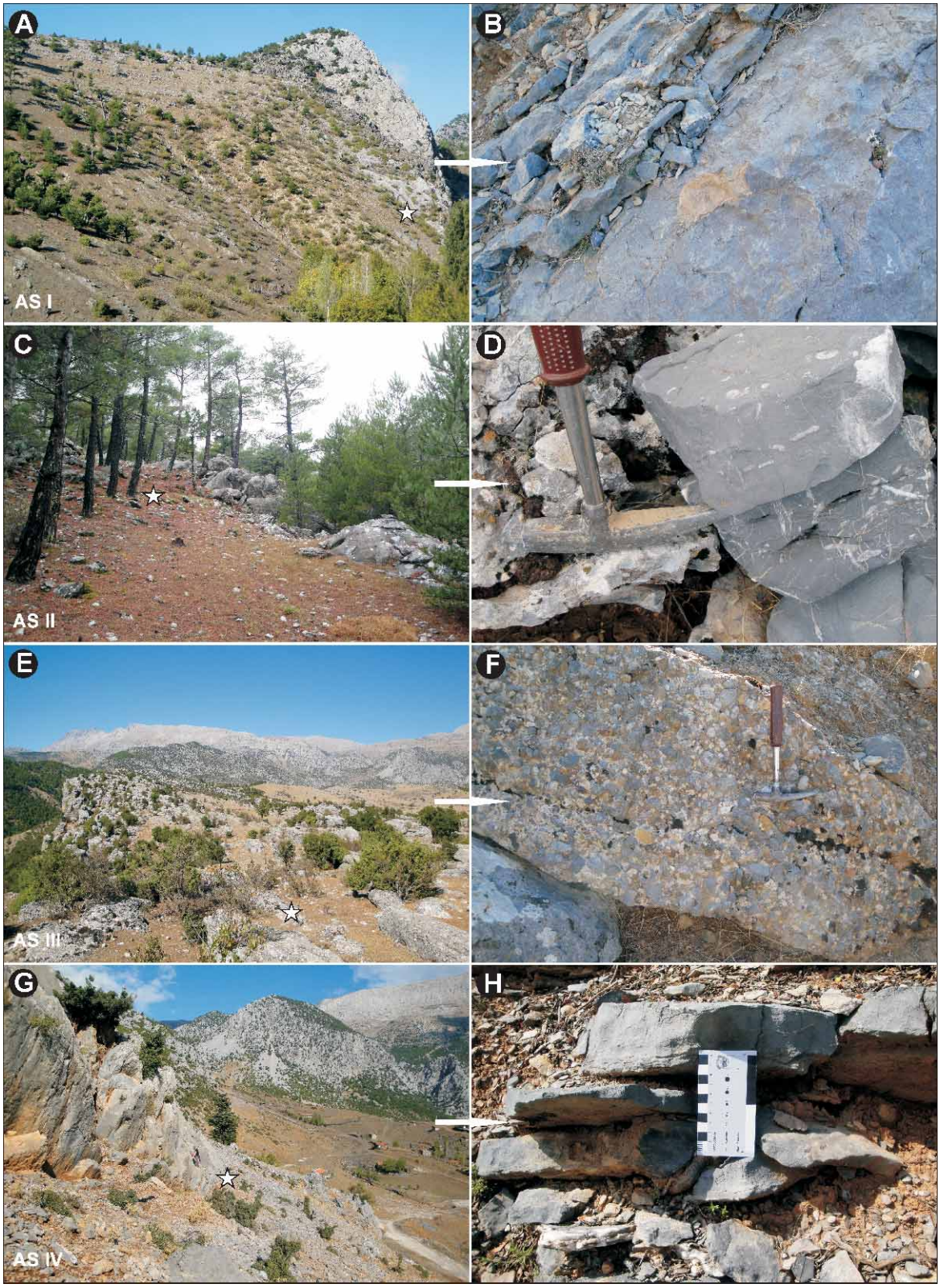

Fig. 3. Localities and detailed views on the *Kasimlarceltites* layers within shallow water carbonates from the Kasımlar Formation of the sections around Aşağıyaylabel (AS I, AS II, AS III, AS IV). **A** — The locality Aşağıyaylabel 1 (AS I); **B** — Detail of the *Kasimlarceltites* acme zone at AS I, base of the Kasımlar Formation; **C** — The locality Aşağıyaylabel 2 (AS II); **D** — Detail of the *Kasimlarceltites* acme zone at AS II; **E** — The locality Aşağıyaylabel 3 (AS III) within Cenozoic (middle Miocene) conglomerates of the Köprüçay Formation; **F** — Detail of the conglomerates comprising Triassic blocks with *Kasimlarceltites* accumulations; **G** — The locality Aşağıyaylabel 4 (AS IV); **H** — Detail of the *Kasimlarceltites* acme zone at AS IV, base of the Kasımlar Formation.

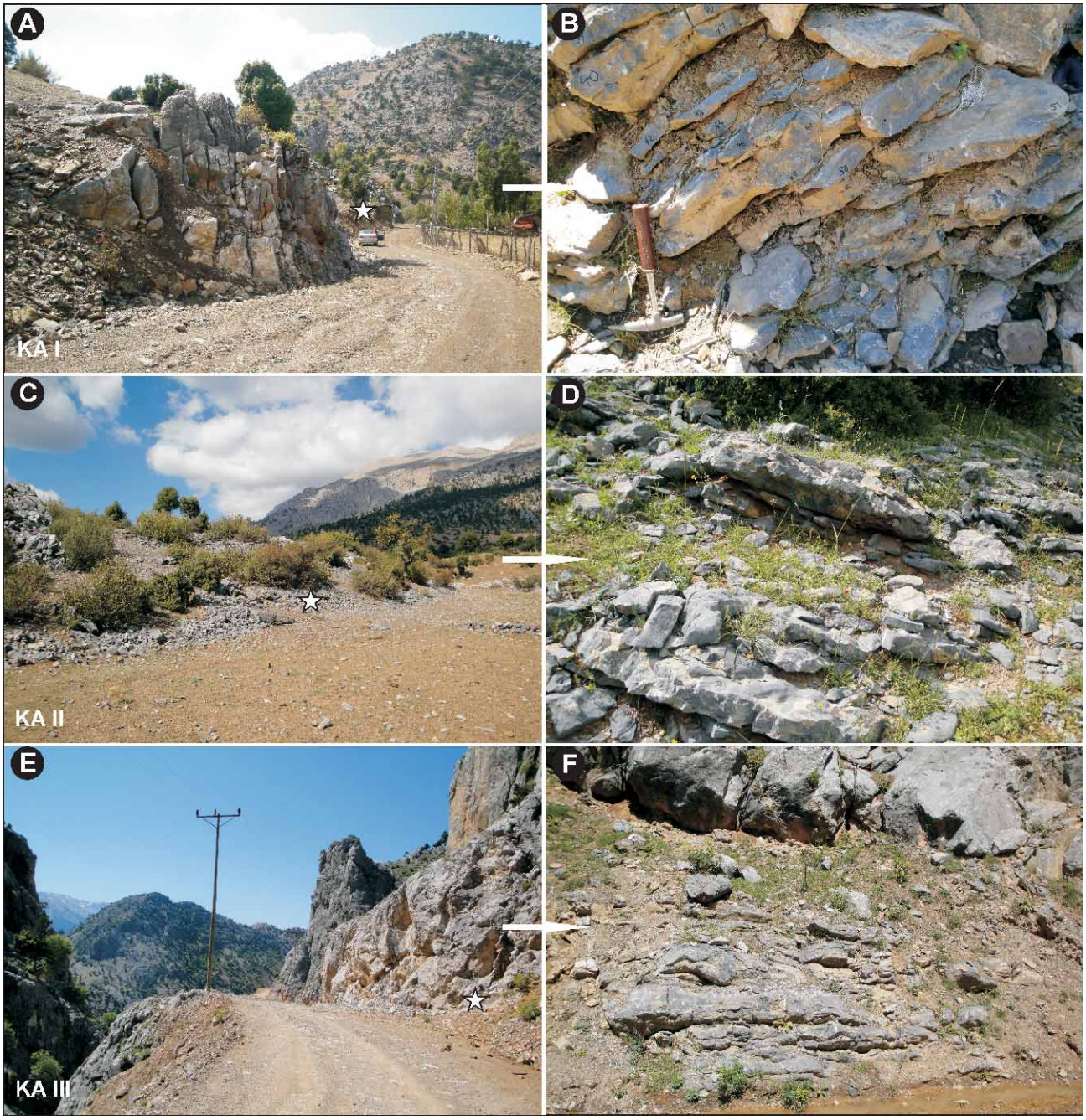

Fig. 4. Localities and detailed views of the *Kasimlarceltites* layers within shallow water carbonates from the Kasımlar Formation of the sections around Karapınar (KA I, KA II, KA III). **A** — The locality Karapınar 1 (KA I); **B** — Detail of the *Kasimlarceltites* acme zone at KA I, base of the Kasımlar Formation; **C** — The locality Karapınar 2 (KA II); **D** — Detail of the *Kasimlarceltites* acme zone at KA II, middle part of the Kasımlar Formation; **E** — The locality Karapınar 3 (KA III); **F** — Detail of the *Kasimlarceltites* acme zone at KA III, base of the Kasımlar Formation.

Formation as Julian 2 (*Austrotrachyceras austriacum* Zone). A hiatus between this top and the overlying Kasımlar Formation cannot be excluded for all sections.

The overlying Kasımlar Formation can be divided into three 'members': a carbonate member, a marlstone member, and a shale member (Lukeneder et al. 2012). The carbonate member starts with dark-grey to black, thin-bedded limestones containing ammonoid-rich beds with a nearly monospecific assemblage of *Kasimlarceltites* and very rare *Sirenites,* represented by floatstones of latest Early Carnian age (Julian 2/II; Fig. 2). Towards the top thick slump breccias follow; they contain up to meter-sized patch-reef blocks together with small ammonoid coquinas and filament-limestone components. The overlying well-bedded (cm–dm thick) peloidal filament-wackestone with Lower Carnian conodonts (e.g. *Gladigondolella tethydis* and *Metapolygnathus*) and an am-

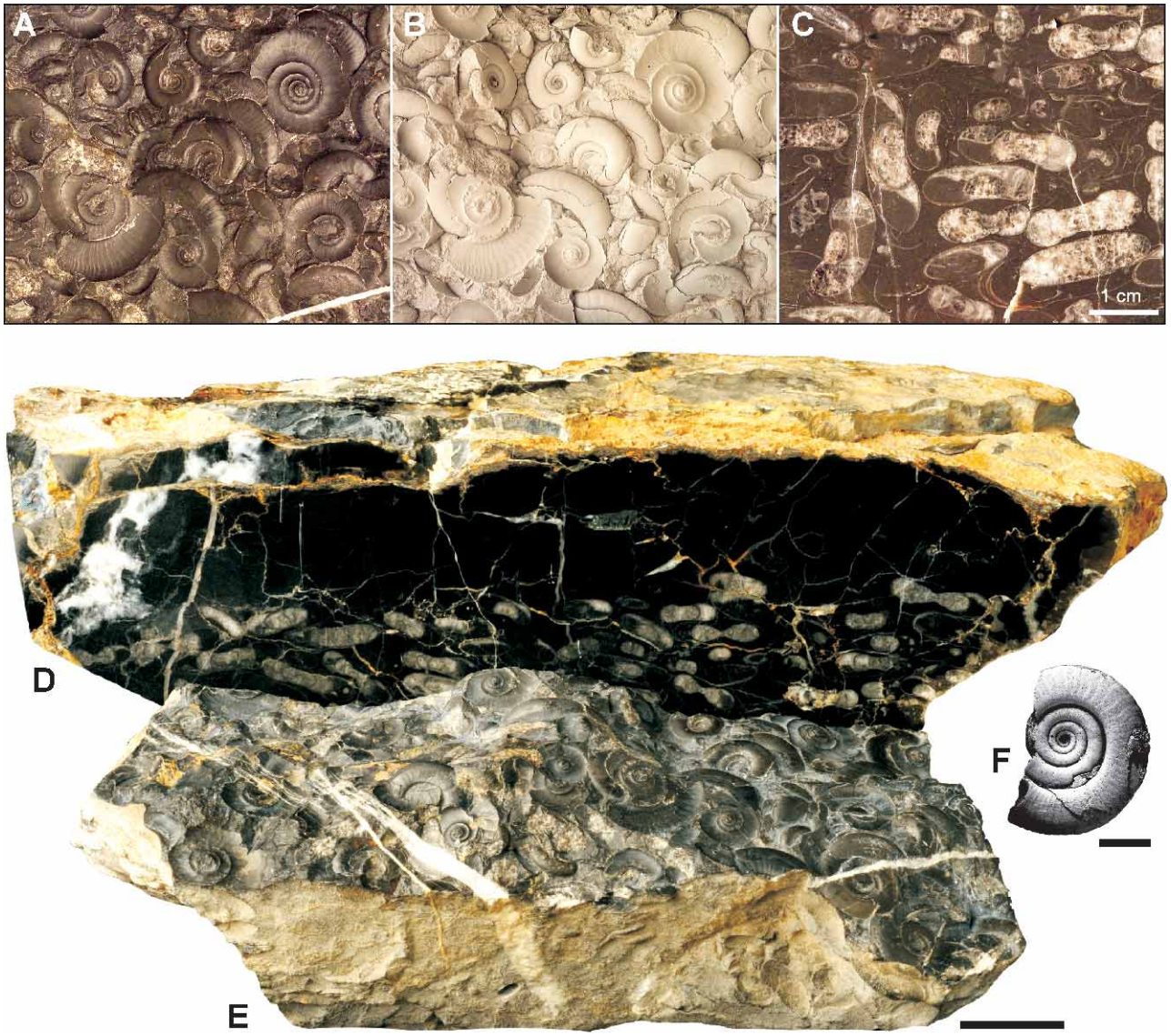

Fig. 5. A — Surface of an accumulation layer of *Kasimlarceltites*, uncoated, NHMW 2012/0133/0558; **B** — Same specimen coated with ammonium chloride, NHMW 2012/0133/0558; **C** — Top-to-bottom thin section of the same layer with densely packed ammonoid shells, NHMW 2012/0133/0559; **D** — Polished slice of an ammonoid accumulation layer at section AS IV — block 1–slice C (89 mm, frontal view), NHMW 2014/0091/0001; **E** — Ammonoid accumulation surface from section AS IV, NHMW 2012/0133/0558; **F** — *Kasimlarceltites krystyni*, lateral view, holotype, NHMW 2012/0133/0014. Kasımlar Formation, Carbonate member Unit A, *Austrotrachyceras austriacum* Zone (Julian 2). Each scale bar represents 1 cm.

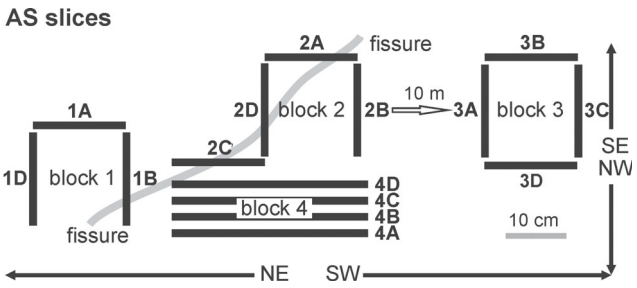

Fig. 6. Terminology and orientation of frontal and orthogonal sections measured from the locality Aşağıyaylabel I, with indicated present-days cardinal directions for blocks AS I, AS II, AS III and AS IV.

monoid fauna dominated by the genera *Neoprotrachyceras* and *Anasirenites* are of latest Early Carnian age (*Anasirenites* level of Julian 2/IIb). The bioturbated matrix contains juvenile halobiid bivalves, sponge spicules, radiolaria, peloids, and planktic crinoids (= *Osteocrinus* sp.).

The interval with the comprising *Kasimlarceltites* acme zone (lowermost Carbonate member) represents the latest Early Carnian (Julian 2 — Lukeneder & Lukeneder 2014; Fig. 2).

The *Kasimlarceltites* mass occurrence

The *Kasimlarceltites* mass-occurrence resp. acme zone is quite common in the area around Aşağıyaylabel and Karapınar.

For a detailed data set of the Aşağıyaylabel area (AS Ia, AS Ib, AS II, AS III) and the Karapınar area (KA I, KA II, KA III) on lithology, microfacies, geochemistry, geophysics, fossil content and environment see Table 1. The standard Microfacies zones (i.e. SMF zones) are in accordance with Flügel (1978, 2004; see also Carrillat & Martini 2009) and Lukeneder et al. (2012).

The Aşağıyaylabel (Kartoz) area

Locality: Aşağıyaylabel Ia, AS Ia (Figs. 1, 2, 3A–B; Table 1)
Lithology: Dark grey to black limestone
Interpretation: Debris flow, event bed

Locality: Aşağıyaylabel Ib, AS Ib (Figs. 1, 2, 3A; Table 1)
Lithology: Dark grey to black limestone
Interpretation: Debris flow

Locality: Aşağıyaylabel II, AS II (Figs. 1, 2, 3C–D; Table 1)
Lithology: Dark grey to black limestone
Interpretation: Debris flow, event bed

Locality: Aşağıyaylabel III, AS III (Figs. 1, 3E–F; Table 1)
Lithology: Dark grey to black limestone
Interpretation: Primary debris flow, secondary fan-delta conglomerates

Locality: Aşağıyaylabel IV, AS IV (Figs. 1, 2, 3G–H; Table 1)
Lithology: Dark grey to black limestone
Interpretation: Turbidite, event bed

The Karapınar (Yukarıyalabel) area

Locality: Karapınar I, KA I (Figs. 1, 2, 4A–B; Table 1)
Lithology: Dark grey to black limestone
Interpretation: Debris flow, event bed

Locality: Karapınar II, KA II (Figs. 1, 2, 4C–D; Table 1)
Lithology: Dark grey to black limestone
Interpretation: Debris flow, event bed

Locality: Karapınar III, KA III (Figs. 1, 2, 4E–F; Table 1)
Lithology: Dark grey to black limestones
Interpretation: Debris flow, event bed.

The *Kasimlarceltites* mass occurrence as an abundance zone

An abundance zone or acme zone is a stratum or body in which the abundance of a particular taxon or specified group of taxa is significantly greater than is usual in the adjacent parts of the section (Salvador 1994; Murphy & Salvador 1999). Its boundaries are made of biohorizons and the name is given by the abundant taxon or taxa (Lukeneder 2003b). Biohorizons are, for example, characterized by a sharp and significant biostratigraphic change within the fossil assemblage and/or the change of frequency of its members (see Salvador 1994; Steininger & Piller 1999). The latter authors recommended the term biohorizon to be used instead of the terms 'surface', 'level', 'marker' and 'datum planes'. Such biohorizons are of great importance for lateral correlation over wide distances. Densely fossiliferous layers were also termed as 'shell beds', 'coquinas', 'concentration-*Lagerstätten*', 'lumachelles', 'bioclastic limestones' and 'bioclastic beds' (Brett & Seilacher 1991; Kidwell 1991a,b; Martin 1999).

Patterns which lead to beds with a notable abundance of ammonoid shells have been called 'inter-regional mass occurrences' or 'stray occurrences' (Kemper et al. 1981). Such abundance zones are of exceptional value for intra-regional correlation in the Triassic.

An Upper Triassic monotonous ammonoid assemblage representing a thickness of at least one single bed up to a few meters, were reported and taxonomically described by Lukeneder et al. (2012 — 'ammonite floatstones with *Orthoceltites*'; *Orthoceltites* = old synonym of *Kasimlarceltites*) and Lukeneder & Lukeneder (2014 — '*Kasimlarceltites* mass occurrence').

At the investigated Aşağıyaylabel (AS I–IV) and Kasımlar (KA I–III) sections the *Kasimlarceltites* ammonoid abundance zone (characterized by abundance or mass occurrence of ammonoids) could be detected for the first time. The names of the separated beds were given following the dominating genus *Kasimlarceltites*.

The *Kasimlarceltites* acme zone starts at every section from Aşağıyaylabel and Karapınar directly above the shallow water carbonates of the Kartoz Formation (Fig. 2). At AS Ia and AS IV, the *Kasimlarceltites* acme zone is capped by an interval of debris flow deposits comprising Cipit boulders (Lukeneder et al. 2012). At the Karapınar sections, the upper edge of the sections is not visible, hence ending within the *Kasimlarceltites* beds. The acme zone appears with deviant ranges or thickness in distinct localities (Fig. 2; Table 1). It occurs at the sections AS Ia with 1.8 m, at AS Ib with 8.0 m, at AS II in single blocks, at AS III within Cenozoic conglomerates (Deynoux et al. 2005) as reworked blocks, and at AS IV with 4.0 m. The acme zone sections at Karapınar appear at KA I with 6.0 m, at KA II with 16.5 m and at KA III with 5.0 m. The most undisturbed and entire section occurs at KA II. Other sections (e.g. AS Ia, AS IV, KA I, KA III) are characterized by tectonics or seem to be affected by more or less strong shearing mechanisms.

Biostratinomy and taphonomy

The biostratinomy is defined as the sum of environmental factors that affect organic remains between death and the final burial or embedding (Müller 1963; Brett & Baird 1986; Martin 1999). Biostratinomy is thus a very important part of work in taphonomy, the study of the entire *post mortem* history of organic remains resulting in fossil material (Fernández-López & Fernández-Jalvo 2002; Fernández-López 2007).

The taphonomic investigations of fossil cephalopod assemblages provide insight, not only into the autecology of these organisms, but also into their paleoenvironment and paleocommunity structure (Brett & Baird 1986; Allison & Briggs 1991; Brett & Seilacher 1991; Bottjer et al. 1995).

Table 1: Parameters of the *Kasimlarceltites* Abundance Zone and measured blocks at different localities in the Aşağıyaylabel and Karapınar area. Data are measured within this study for the first time.

Parameters	*Kasimlarceltites* abundance zones at different localities in the Aşağıyaylabel and Karapınar area							
	AS Ia	**AS Ib**	**AS II**	**AS III**	**AS IV**	**KA I**	**KA II**	**KA III**
Geography, geology and stratigraphy								
Locality	Aşağıyaylabel N 37°33'05" E 31°18'14"	Aşağıyaylabel N 37°33'05" E 31°18'14"	Aşağıyaylabel N 37° 32' 47" E 31°18'23"	Aşağıyaylabel N 37°32'13" E 31°17'32"	Aşağıyaylabel N 37°55'48" E 31°30'05"	Karapınar N 37°57'69" E 31°29'12"	Karapınar N 37°57'63" E 31°29'20"	Karapınar N 37°57'55" E 31°28'91"
Dipping [°]	50/075	single blocks	single blocks	single blocks	70/340	70/075	20/010	50/280
Thickness of acme [m]	≈1.8	≈8.0	single blocks	single blocks in Cenozoic (Miocene) conglomerates	≈4.0	≈6.0	≈16.5	≈5.0
Lateral distribution [m]	ammonoids layers detected over 30 m	ammonoids boulders detected over 30 m	ammonoids boulders detected over 50 m	boulder field, 500 m	ammonoids layers detected over 50 m	ammonoids layers detected over 20 m	ammonoids layers detected over 50 m	ammonoids layers detected over 20 m
Biostratigraphy	early Carnian, Julian 2, *Austrotrachyceras austriacum* Zone	early Carnian, Julian 2, *Austrotrachyceras austriacum* Zone	early Carnian, Julian 2, *Austrotrachyceras austriacum* Zone	early Carnian, Julian 2, *Austrotrachyceras austriacum* Zone	early Carnian, Julian 2, *Austrotrachyceras austriacum* Zone	early Carnian, Julian 2, *Austrotrachyceras austriacum* Zone	early Carnian, Julian 2, *Austrotrachyceras austriacum* Zone	early Carnian, Julian 2, *Austrotrachyceras austriacum* Zone
Age [Ma]	≈234	≈234	≈234	15 Ma (boulder ≈234)	≈234	≈234	≈234	≈234
Lithological unit	Kasımlar Formation, Carbonate member, Unit A	Kasımlar Formation, Carbonate member, Unit B	Kasımlar Formation, Carbonate member, Unit B	Cenozoic Köprüçay Formation	Kasımlar Formation, Carbonate member, Unit A	Kasımlar Formation, Carbonate member, Unit A	Kasımlar Formation, Carbonate member, Unit A	Kasımlar Formation, Carbonate member, Unit A
Sedimentology								
Sediment classification of accumulation bed	bioclastic pack- to floatstone	bioclastic rudstones with intra- and extraclast breccias	bioclastic pack- to floatstone, rudstone	bioclastic pack- to floatstone, rudstone	bioclastic packstone	ammonoid-bivalve-bioclastic pack- to floatstone	bioclastic (radiolaria) floatstone	bioclastic floatstone
Standard microfacies types, SMF zone	SMF 12	SMF 6	SMF 12/6	SMF 12/6	SMF 12	SMF 12	SMF 12	SMF 12
Sediment structure/fabrics	vertical neptunian dykes	no orientation of bioclasts	orientation / no orientation	no orientation of bioclasts	orientation of bioclasts	orientation of bioclasts	≈ horizontal weakly oblique orientation	slightly oblique
Base of bed	erosional wavy	Cipit boulders	boulder	boulder	straight	stylolitic base	straight	straight
Top of bed	erosional wavy	Cipit boulders	boulder	boulder	straight	straight	straight	straight
Bioturbation	yes, frequent	yes, frequent	yes, distinct	present	distinct to frequently	frequent	frequent	present
Sediment classification below the accumulation bed	bioclastic packstone (AS 3)	bioclastic floatstone to packstone (AS 7)	boulder	boulder	bioclastic floatstones (AS 7)	peloidal pack- to floatstone, silt to fine sand (KA I/9)	peloidal pack- to floatstone, silt (KAII ZBb)	peloidal pack- to floatstone, silt (KA III)
Sediment classification above the accumulation bed	bioclastic floatstone to packstone (AS 7)	bioclastic floatstone to packstone (AS 19)	boulder	boulder	bioclastic floatstones AS (9)	peloidal pack- to floatstone, silt to fine sand (KA I/11)	peloidal pack- to floatstone, silt (KA II)	peloidal pack- to floatstone, silt (KA III)
Geochemistry and geophysics								
Grey scale 0–255	130.5	98.5	124	113	105.5	93	96.5	112
$CaCO_3$ [%]	91.8	89.8	90.6	88.9	91.4	91.7	90.9	89.7
Colour	dark grey to black	dark grey to black	dark grey to black	dark grey to black	dark grey to black	dark grey to black	dark grey to black	dark grey to black
TOC [%]	0.132	0.203	–	–	–	–	–	–
S [%]	0.03	0.11	–	–	–	–	–	–
Pyrite	frequent, framboidal	frequent, framboidal	frequent, framboidal	frequent, framboidal	frequent, framboidal	frequent, framboidal	frequent, framboidal	frequent, framboidal and cubes
Gamma ray [cps]	27	15	21	26	28	135	19	23
Susceptibility SI 10^{-6}	55	52	49	57	20	66	43	47
$\delta^{13}C$ [‰]	2.10	1.70	–	–	1.94	2.09	2.07	–
$\delta^{18}O$ [‰]	–8.80	–8.80	–	–	– 6.65	–7.16	–7.17	–

Sediments of the lower Upper Triassic (Carnian) of the Kasımlar Formation appear in the lower part with well preserved and mostly entire (>95 %) ammonoid specimens (Fig. 5). The distinct ammonoid shell concentration beds within single logs and different localities (i.e. Aşağıyaylabel and Karapınar) differ in lateral distribution, thickness, sedimentological features, packing of shells, diversity of organisms, alignment and taphonomic processes (Figs. 6, 7, 9, 10; Tables 1, 2, 3; see also Fürsich & Pandey 1999).

The ammonoids are tiny with a maximum diameter of 33 mm. They show an involute more spheroidal shape and are accumulated in the beds AS Ia— beds 4, 6; AS IV — bed 8; KA I — beds 10, 12; KA II — beds 2, 11, 122; KA III — bed 8. Less than 5 % of those accumulated ammonoids are

Table 1: *Continued.*

Parameters	***Kasimlarceltites* abundance zones at different localities in the Aşağıyaylabel and Karapınar area**							
	AS Ia	**AS Ib**	**AS II**	**AS III**	**AS IV**	**KA I**	**KA II**	**KA III**
Taphonomy								
Shell infill	matrix in body chamber within numerous specimens, shallow water fragments in body chamber, secondary calcite in phragmocones	matrix in body chamber, peloids and shallow water fragments in body chamber, secondary calcite in phragmocones	matrix in body chamber, frequent pelloids to silts, secondary calcite in phragmocones	matrix in body chamber, frequent pelloids to silts, secondary calcite in phragmocones	matrix in body chamber, frequent pelloids, silts to very fine sand, secondary calcite in phragmocones	matrix in body chamber, frequent pelloids, silts to very fine sand, juvenile ammonites, secondary calcite in phragmocones	matrix in body-chamber, frequent pelloids, silts, juvenile ammonites, secondary calcite in phragmocones	matrix in body chamber, frequent pelloids, silts, juvenile ammonites, secondary calcite in phragmocones
Shell orientation alignment	inhomogenous and heterogenous within bed, present in parts of layer, horizontal to oblique	absent, oblique	present to absent, horizontal to oblique	absent, oblique, nesting	present, weakly oblique	present, weakly oblique	present, weakly oblique	present, weakly oblique
Fabric/packing	dense, partly disorientated, partly aligned	dense	dense	loosely to dense	dense	dense	dense only at base of layer	dense in the mid of layer
Sorting of shells	present	absent	absent	absent	good	absent	bad	absent
Geopetal structures	slightly divergent; in top of body chambers	dislocated against each other, in body chambers	dislocated against each other, in body chambers	dislocated against each other, in body chambers	slightly divergent; in top of body chambers	oblique, dislocated against each other, in body chambers	dislocated against each other, in body chambers	slightly dislocated against each other
Biodegradation	no soft parts or aptychi, septal necks visible in thin sections	no soft parts or aptychi, septal necks visible in thin sections	no soft parts or aptychi, septal necks visible in thin sections	no soft parts or aptychi, septal necks visible in thin sections	no soft parts or aptychi, septal necks visible in thin sections	no soft parts or aptychi, septal necks visible in thin sections	no soft parts or aptychi, septal necks visible in thin sections	no soft parts or aptychi, septal necks visible in thin sections
Incrustation	absent	absent	absent	absent	absent	absent	absent	absent
Bioerosion	absent	absent	absent	absent	absent	absent	absent	absent
Transport	no abrasion, but frequent breakage due to transport	strong transport, redeposition, mixed shallow water faunas (patch reefs), deeper ramp facies and pelagic basin elements, no abrasion, but frequent breakage in ammonoids	strong transport, redeposition, mixed shallow water faunas (patch reefs), deeper ramp facies and pelagic basin elements, no abrasion, but frequent breakage in ammonoids	strong transport, redeposition, mixed shallow water faunas (patch reefs), deeper ramp facies and pelagic basin elements, no abrasion, but frequent breakage in ammonoids	strong transport, redeposition, coquina on top of laminated silt layers	strong transport, redeposition, frequent breakage in ammonoids	strong transport, redeposition, rare breakage in ammonoids	strong transport, redeposition, rare breakage in ammonoids
Dissolution of shell	stylolites and pressure seems frequent	pressure seems frequent	absent	absent	stylolites and pressure seems frequent	rare stylolites	stylolites, pressure seems frequent	stylolites
Diagenetical deformation and compaction	on top of beds	present	absent to strong	strong	absent to strong	present	rare	rare
Depositional area	mid-outer ramp, slope to basin	outer ramp to slope	outer ramp to slope	primary: outer ramp to slope; secondary: conglomerate field	mid-outer ramp, slope to basin	mid-outer ramp, slope to basin	mid-outer ramp, slope to basin	mid-outer ramp, slope to basin
Interpretation	debris flow, event bed	debris flow	debris flow	debris flow	turbidity, event bed	debris flow, event bed	debris flow, event bed	debris flow, event bed
Faunal assemblage								
Genus	*Kasimlarceltites*	*Kasimlarceltites*	*Kasimlarceltites*	*Kasimlarceltites*	*Kasimlarceltites*	*Kasimlarceltites*	*Kasimlarceltites*	*Kasimlarceltites*
Quantity	>95 %	≈40–90 %	≈50–90 %	>50–90 %	>95 %	50 %	>95 %	>95 %
Ratio infauna	>95 %	40–90 %	50–90 %	>50–90 %	>95 %	50 %	>95 %	>95 %
Acme zone [m]	1.8	≈8.0	boulders	blocks and boulders	≈4.0	≈6.0	≈16.5	≈5.0
Accumulation layers	AS Ia/4, 6	AS Ib/18	AS Ia/18 boulders	blocks and boulders	AS IV/8	KA I/10 (12)	KA II/2, 11, 16	KA III/8
Event bed thickness [m]	≈0.1	≈8.0	boulders	blocks and boulders	0.1–0.15, in the middle part 0.05 shell coquina	0.03–0.05	0.03–0.05	0.05–0.1
Ontogenetical stages	juvenile & adult	ammonitellae, juvenile & adult	ammonitellae, juvenile & adult	ammonitellae, juvenile & adult	juvenile & adult	ammonitellae, juvenile & adult	ammonitellae, juvenile & adult	ammonitellae, juvenile & adult
Size range cm min–max	0.5–3.3	0.01–3.3	0.01–3.3	0.001–3.3	0.001–2	0.001–2.2	0.001–2.5	0.001–2.2
Shell material	secondary calcite	secondary calcite	secondary calcite	secondary calcite	secondary calcite	secondary calcite	secondary calcite	secondary calcite
Accompanying macro-fauna	ammonoids (*Sirenites* sp.), gastropods (omphaloptyychids) bivalves (halobiids), sponges	ammonoids (*Sirenites* sp.), gastropods (omphaloptyychids) bivalves (halobiids), sponges (chaetitids), corals, echinoids, crinoids	ammonoids (*Sirenites* sp.), gastropods (omphaloptyychids) bivalves (halobiids), sponges (chaetitids), corals, echinoids, crinoids	ammonoids (*Sirenites* sp.), gastropods (omphaloptyychids) bivalves (halobiids), sponges (chaetitids), corals, echinoids, crinoids	rare bivalves	50 % *Sirenites* sp., bivalves, rare gastropods, rare sponges	bivalves, rare gastropods	bivalves, rare gastropods
Accompanying micro-fauna	ostracods, foraminifera, radiolaria, conodonts	ostracods, foraminifera, radiolaria, conodonts	ostracods, foraminifera, radiolaria, conodonts	ostracods, foraminifera, radiolaria, conodonts	ostracods, foraminifera, radiolaria, conodonts	ostracods, foraminifera, radiolaria, conodonts	ostracods, foraminifera, radiolaria-bloom, conodonts	ostracods, foraminifera, radiolaria, conodonts

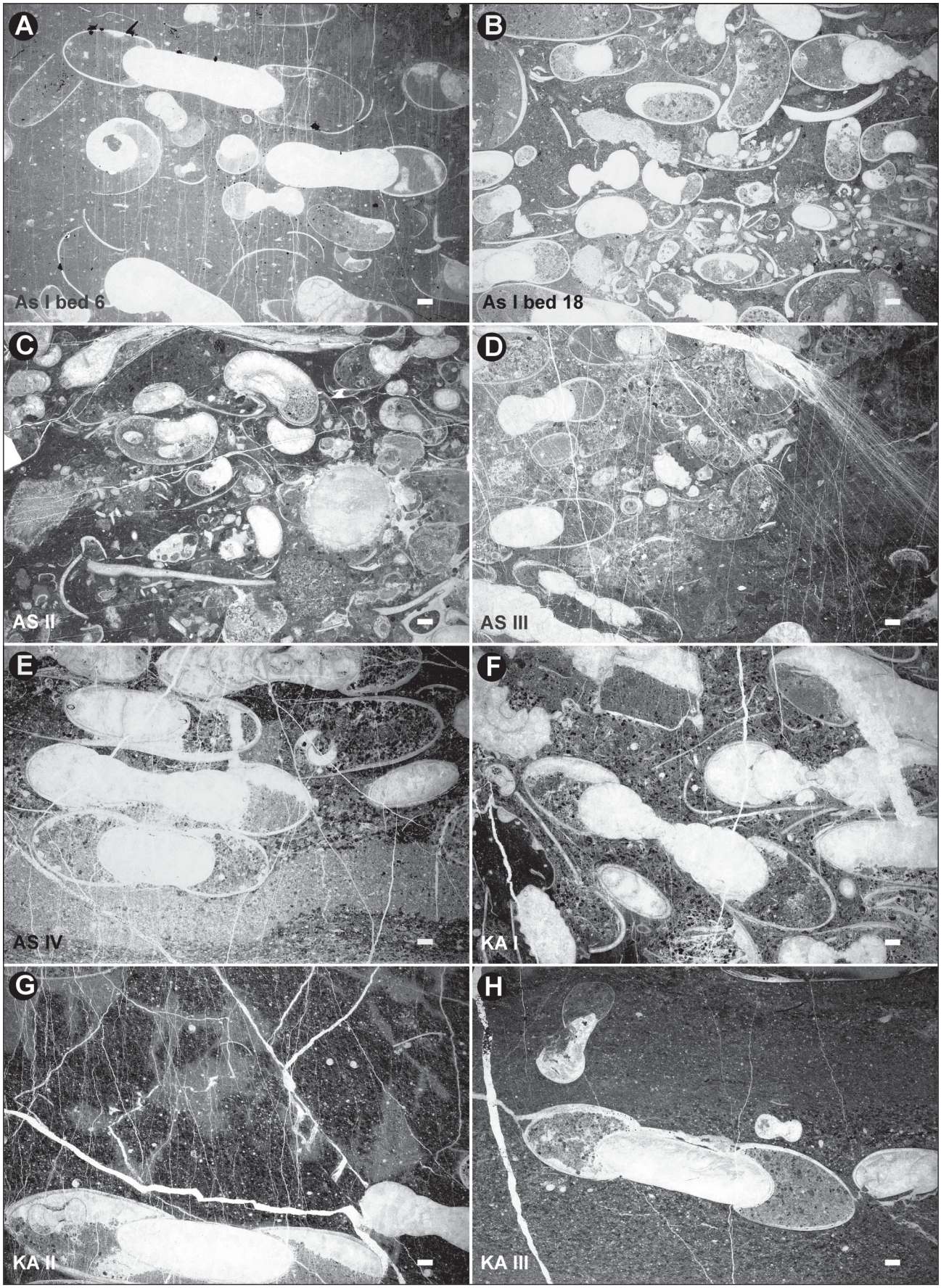
A
As I bed 6
B
As I bed 18
C
AS II
D
AS III
E
AS IV
F
KA I
G
KA II
H
KA III

preserved only with fragmentation. Small accumulated ammonoids of all ontogenetic stages (i.e. *Kasimlarceltites*) as well as shell fragments in body chambers of adjacent large ammonoids can be found within the above mentioned beds, which might hint at the effect of agglomeration and comminution by dense sediment flows with a laminar internal flow. Both, straight shells (e.g. *Atractites*) and also planispiral coiled shells (e.g. *Kasimlarceltites*, *Sirenites*, *Neoprotrachyceras*) are present within the *Kasimlarceltites* acme zone. Erosional features, as described by Fernández-López (2007) and encrustation of ammonoids are absent. Whilst in some thin and distinct layers ammonoids are accumulated in masses with an almost horizontal alignment (Figs. 8–10), ammonoids are less abundant in the limestone beds between the ammonoid mass occurrence beds (Figs. 5, 6, 9).

In accumulated mixed assemblages (i.e. autochthonous, parautochthonous and allochthonous; Martin 1999), detected at the Aşağıyaylabel outcrops AS Ia (Lukeneder et al. 2012), AS II–IV and the Karapınar KA I–III sections, females (= macroconchs) and corresponding males (= microconchs) are found together. In most cases even ammonitellae, juvenile and adult stages are detected in the same layers. Some ammonoid specimens show different sediment-infillings within the body chamber (coarser material) compared to the surrounding finer limestone chamber ('normal' sedimentation = ambient sediment). All of these facts might point to post-mortem, biostratinomic mixing of ecologically age-separated populations as discussed by Olóriz (2000) and Olóriz & Villaseñor (2010). Due to the long body chamber (i.e. mesodome-longidome) in *Kasimlarceltites*, geopetal structures (i.e. sparry calcite on top) are also observable in numerous body chambers (see Olivero 2007; cf. Seilacher 1968), hence body chambers were not entirely filled. Geopetal structures are generally aligned in almost identical directions. No serious mixture and dislocation of geopetal alignments occurs (Figs. 7, 9). Furthermore, the mixed assemblages comprise a considerable amount of bivalves, gastropods, sponges and corals from shallower environments from a nearby platform or upper ramp (Lukeneder et al. 2012).

Ammonoid shell alignment

Angles and orientation of shells and body chambers (both in respect to the horizontal block surface) from 20 blocks with 34

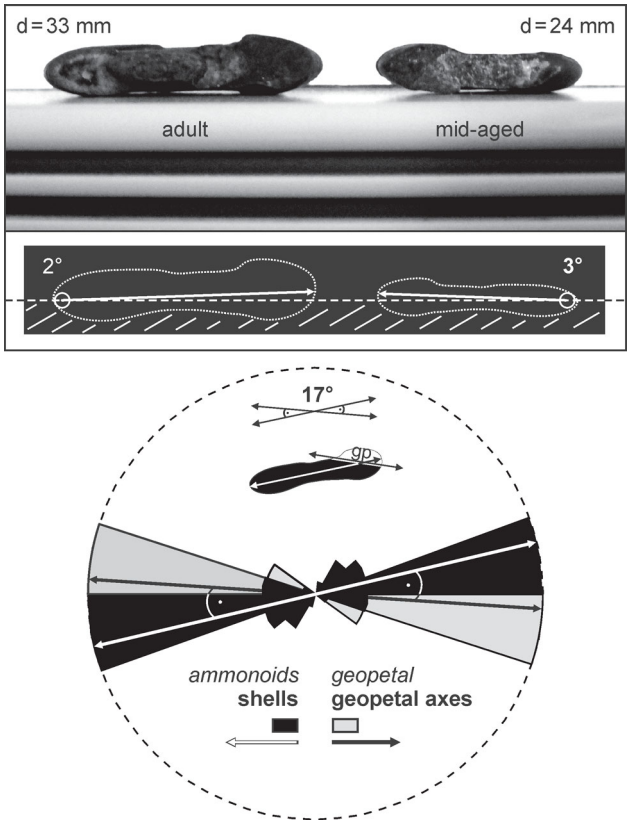

Fig. 8. A — Primary angles in shell axes (i.e. 2°–3°) caused by the ontogenetic variation of whorl breadth in mid-aged and adult *Kasimlarceltites* (adult = holotype, NHMW 2012/0133/0014); **B** — Shell axes (black pies, white arrow) and geopetal axes (grey pies, black arrow) of *Kasimlarceltites* and *Sirenites* within a sample KA II — block 4 (sections D–E–F).

Fig. 7. Thin-section photographs of accumulation layers and facies from the Kasımlar Formation at Aşağıyaylabel and Karapınar. **A–H** — Note the well preserved shell geometry indicating very early cementation (i.e. early selective lithification): A — Bioclastic floatstone with the abundant ammonoid *Kasimlarceltites* and halobiids, accompanied by rare gastropods. The ammonoids and gastropods are filled with coarse sparry calcite floating in micritic matrix, base of *Kasimlarceltites* Formation, AS I — bed 6, NHMW 2012/0133/0560; B–C — Very irregular packing = "injection" of heterometric bioclasts (**B**), and the same but with larger heterometric range (**C**); B — Bioclastic floatstone-packstone, characteristic sponge-accentuated Cipit facies dominated by *Kasimlarceltites* and sponges, accompanied by *Sirenites*, gastropods and corals, Kasımlar Formation, AS I — bed 18, NHMW 2012/0133/0561; C — Bioclastic floatstone-packstone, sponge-accentuated Cipit facies dominated by *Kasimlarceltites* and sponges, accompanied by gastropods and corals, peloidal matrix, Kasımlar Formation, AS II, NHMW 2014/0094/0001; D — Allochthonous block with mixed packstone (left) and floatstone (right) areas, dominated by *Kasimlarceltites* and sponges, accompanied by *Sirenites*, gastropods and corals; found within the Cenozoic (middle Miocene) conglomerates, Köprüçay Formation, AS III, NHMW 2014/0095/0001; shelter effects favouring very dense packing; E — Bioclastic packstones with the abundant ammonoid *Kasimlarceltites* above laminated, peloidal packstone layers, base of Kasımlar Formation AS IV — bed 8, NHMW 2014/0091/0008; sheltering by fragmented body chamber infilled by a very fine comminute matrix; F — Bioclastic packstones with the abundant ammonoids *Kasimlarceltites* and *Sirenites*, peloidal matrix, base of Kasımlar Formation, KA I, NHMW 2014/0092/0003; comminute, bioclastic matrix and reworked ammonoids; G — Bioclastic wackestone with a redeposited, floated *Kasimlarceltites* shell (note dislocated geopetal structure, different infilling and colour) at the base, matrix contains radiolarian, ammonitellae and juvenile ammonoids, middle Kasımlar Formation, KA II, NHMW 2014/0093/0004; very fine matrix with diagenetic patches; H — Bioclastic wackestone with floated *Kasimlarceltites* shells in the middle, and peloidal packstone at the base, peloidal matrix contains radiolarian, ammonitellae and juvenile ammonoids, base of Kasımlar Formation, KA III, NHMW 2014/0096/0001; geopetals indicate ammonoid reworking. Thin-sections are orientated in upright position. Each scale bars represent 1 mm.

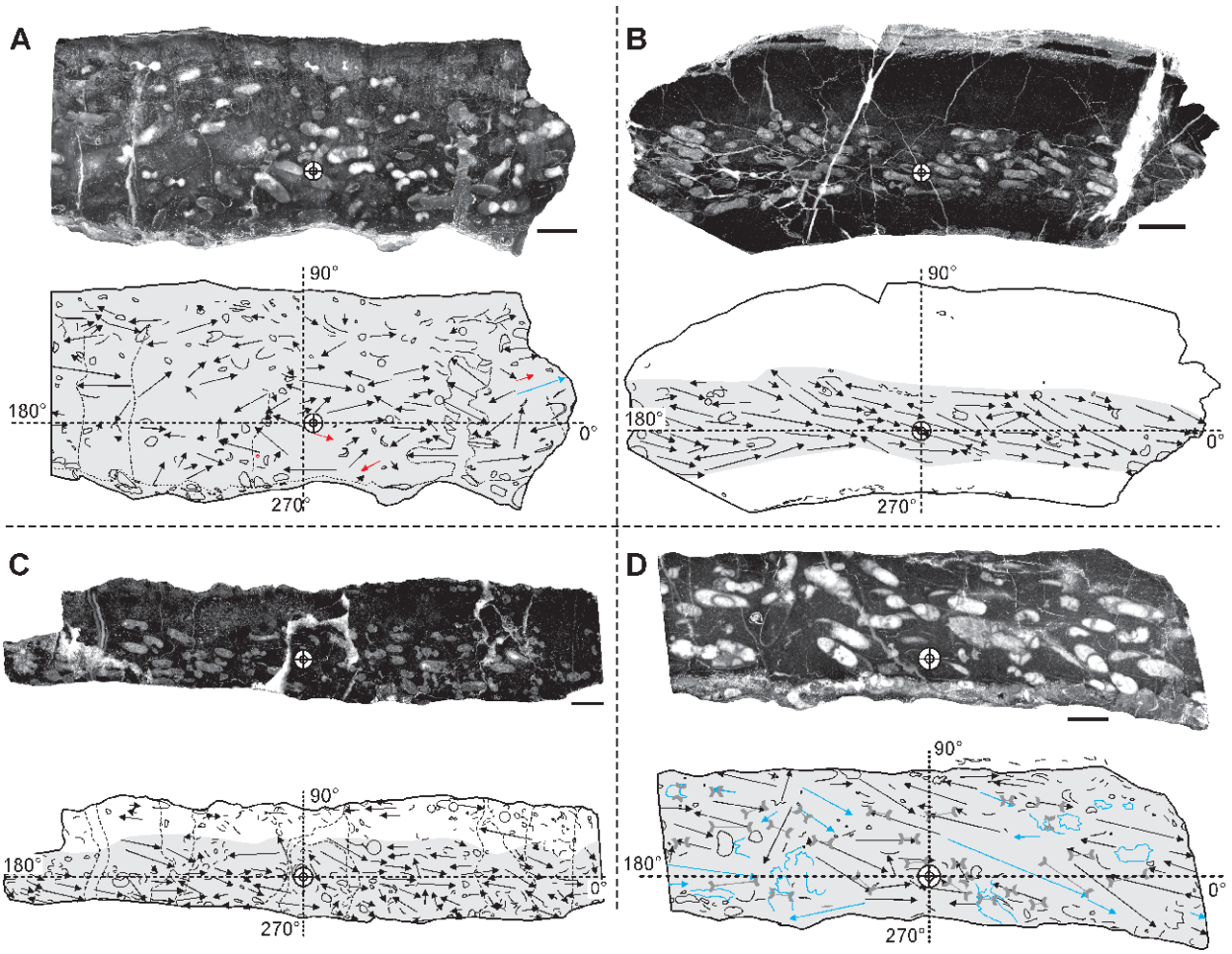

Fig. 9. Ammonoid shell alignment in Carnian blocks from Aşağıyaylabel and Karapınar, with indicated accumulation layers and measurements. **A** — AS I — block 1, slice B (orthogonal view), NHMW 2012/0133/0554; **B** — AS IV — block 1, slice C (89 mm, frontal view), NHMW 2014/0091/0003; **C** — KA I — block 1, slice A (frontal view), NHMW 2014/0092/0001; **D** — KA II — block 4, slice A,B,C (0 degree, frontal view), NHMW 2014/0093/0003. Primary angles in shell axes indicated by arrows, arrowheads directed to the body chamber (= maximum whorl breadth). Sketches (below sections) of the corresponding shell axes (black arrows) of each ammonoid specimen within the event layer (grey shading). Scale bar represents 1 cm.

polished slices from 4 different sites (i.e. AS Ia,b, AS IV, KA I, KA II) were measured in addition with maximal visible diameters on the slices and thin sections. Additional measurements were made on visible geopetal structures. 2367 ammonoid specimens were analysed on slices and sections. Ammonoid shell directions and alignment were not measured in chaotic, transported 'Cipit' boulders from debris flow deposits at AS Ib — bed 18 and within Triassic boulders and blocks incorporated in Cenozoic gravels (Deynoux et al. 2005) of AS III, because they do not mirror the primary mechanism of orientation and transport of ammonoid shells, due to their repeated transport and reorientation.

The most reliable data were obtained from AS I where blocks could be taken orientated (Fig. 6). The front section of the AS I blocks (as taken in the field) is orientated with a direction from NE to SW (NE is left on the block, orientated toward the valley). On a horizontal line, marking the base and surface of the layers and blocks, 0° is located at the right (SW), 90° at the top, 180° at the left (NE) and 270° at the base (Figs. 9, 10). In addition, where possible, slices at 90° (= orthogonal) to the frontal view were performed to get ideas on the three dimensional orientation of the ammonoids in the blocks. To gain the true dip direction (Nichols 2009) of the ammonoid shell 'plane' the calculation needs two different apparent dip measurements (i.e. ammonoid shell axes; Fig. 11). This implies a direction (i.e. only AS I blocks) of the later slices rotated by 90° to a direction of NW (front) to SE (back).

A clear orientation and alignment (Potter & Pettijohn 1977) can be detected in the accumulation layers.

The predominant orientation of shell axes (only AS Ia with cardinal direction) versus the layer base/surface of blocks in frontal and orthogonal slices was analysed at Aşağıyaylabel (Figs. 6, 10, 11, Tables 2, 3).

Frontal
AS Ia, AS IV
Orthogonal
AS Ia, AS IV

Table 2: Results on the biofabric, orientation and size classes of *Kasimlarceltites krystyni* at different localities in the Aşağıyaylabel and Karapınar area, frontal view.

Shell parameters ammonoid shells	**Orientation and size of *Kasimlarceltites* at different localities in the Aşağıyaylabel and Karapınar area, frontal view**							
	AS Ia	**AS Ia**	**AS IV**	**AS IV**	**KA I**	**KA II**	**KA II**	**KA II**
Biofabrics of ammonoid shells								
Block/bed	long block 4, bed 6	block 3, bed 6	blocks 1, 2, bed 8	block 3, –	block 1, bed 10	block 3, –	block 2, –	block 4, –
Orientation in field, front view	left NE SW right	left NE SW right	–	–	–	–	–	–
Slices	1A, 1B, 1C, 1D	3B, 3D	1A 0 mm, 1B 81 mm, 1B thin 85 mm, 1C 89 mm, 2B 100 mm, 2C 240 mm	3A 0 mm, 3B 2 mm, 3C 100 mm, 3D 102 mm	1A 0 mm, 1C 84 mm, 1D 86 mm	3A	2B	4A,B,C 0°
Quantity of angles [n]	853	114	373	36	225	25	27	43
Dominant shell axis	160–180°/340–360° **35.4 %**	140–160°/320–340° **28.75 %**	160–180°/340–360° **43.1 %**	160–180°/340–360° **75.0 %**	160–180°/340–360° **38.7 %**	160–180°/340–360° **32.0 %**	180–200°/000–020° **29.6 %**	160–180°/340–360° **58.1 %**
Dominant angle interval	160–200°/340–020° **59.1 %**	140–200°/320–020° **37.0 %**	160–200°/340–020° **68.1 %**	160–200°/340–020° **97.2 %**	160–200°/340–020° **55.6 %**	160–200°/340–020° **82.0 %**	160–200°/340–020° **34.4 %**	160–200°/340–020° **67.4 %**
Ccomments on axis angle	weakly oblique, unimodal	more oblique, bimodal	weakly oblique, unimodal	weakly oblique, unimodal	weakly oblique, unimodal	weakly oblique, unimodal	more oblique broad, unimodal	weakly oblique, unimodal
Dominant body chamber, up	160–180°, **20.2 %**	140–160°, **23.1 %**	160–180°, **14.2 %**	160–180°, **50.0 %**	160–180°, **16.0 %**	000–020°, **28 %**	140–160°, **14.8 %**	160–180°, **39.5 %**
Dominant body chamber, down	340–360° **15.2 %**	340–360° no dominant range	340–360° **29.0 %**	340–360° **25.0 %**	340–360° **22.7 %**	180–200° **20.0 %**	180–200° **22.2 %**	340–360° **18.6 %**
Comments on body chamber angles	weakly oblique, bimodal	more oblique, unimodal	weakly oblique, unimodal	weakly oblique, unimodal	weakly oblique, bimodal	weakly oblique, bimodal	weakly oblique, bimodal	weakly oblique, unimodal
Size classes and diameters								
Quantity of diameters [n]	853	114	373	36	225	25	27	41
Dominant size class [mm]	4.2–6.2 **24.7 %**	4.2–6.2 **26.3 %**	12.6–14.6 **13.7 %**	8.4–10.4 **16.7 %**	4.2–6.2 **24.4 %**	6.2–8.2 10.4–12.4 both **20 %**	8.4–10.4 **40.7 %**	8.2–10.2 **22.0 %**
Dominant size range [mm]	4.2–10.4 **62.6 %**	4.2–10.4 **65.8 %**	2.1–18.8 **89.0 %**	2.1–23.0 **100 %**	2.1–10.4 **74.7 %**	6.2–20.2 **80 %**	4.2–12.2 **74.1 %**	2.2–18.2 **87.1 %**
Dispersal curve	unimodal, positively skewed	unimodal, positively skewed	broad unimodal– bimodal	broad unimodal– bimodal	unimodal, positively skewed	bimodal	unimodal, positively skewed	unimodal, positively skewed
Mean size [mm]	8.3	7.6	11.7	12.4	7.2	12.6	9.8	11.2
Comment on size	small	small	larger	larger	small	larger	small	larger
Miniumum size [mm]	1.7	1.9	1.1	2.5	1.4	2.4	3.8	2.3
Maximum size [mm]	26.0	18.1	26.2	22.3	18.6	29.0	18.5	26.0
Size range [mm]	24.3	16.2	25.1	19.8	17.2	26.6	14.7	23.7

Within accumulation layers from the Karapınar area the orientation of shell axes (not in cardinal direction) appears in frontal and orthogonal slices (Fig. 10, Tables 2, 3). Layers in KA I can be separated in two parts (accumulation = event layer and above with normal sedimentation), KA II (geopetal axe in body chambers varies in angle section).

Frontal
KA I, KA II
Orthogonal
KA I, KA II

The internal fabric of the accumulation layers (i.e. ammonoid shells) ranges from densely packed, ammonoid shell supported packstones (e.g. AS IV — bed 8; KA I — bed 10) to ammonoid-floatstones (AS Ia — beds 4, 6; Figs. 7). The event layers are heterogeneous, with cases of shell imbrication in parts (see imbrication in turbidite Bouma interval T_a, Bouma et al. 1982; Eberli 1991) and cases of loosely packed or floating specimens in different parts. Even in single blocks, the density diverges from the base, mid part and top of beds (Fig. 9). The matrix infills the body chambers and the space between shells. The imbricated shells show a horizontal or at least low-angle deposition. Vertical or perpendicular ammonoid specimens are extremely rare in accumulation layers of Aşağıyaylabel and Karapınar. An alignment of the biogenic particles (i.e. ammonoid shells) was observed in the majority of the accumulation layers (AS I — beds 4, 6; most beds at KA I, KA II). Although the alignment within most accumulation layers (AS I — beds 4, 6; most beds at KA I, KA II) took place within the sediment, in blocks 1 and 2 (corresponding to the same layer) in AS IV and KA II

Table 3: Results on the biofabric, orientation and size classes of *Kasimlarceltites krystyni* at different localities in the Aşağıyaylabel and and Karapınar area, orthogonal view.

Shell parameters of ammonoid shells	Orientation and size of *Kasimlarceltites* at different localities in the Aşağıyaylabel and Karapınar area, orthogonal view							
	AS Ia	AS IV	KA Ia	KA Ib	KA II	KA II	KA II	KA II
Biofabrics of ammonoid shells								
Block/bed	blocks 1, 2, 3, bed 6	block 3, –	block 1, bed 10	block 1, bed 10	block 3, –	block 2, –	block 4, –	block 4, –
Orientation in field, orthogonal	front NW SE back	– –	–	– –	– –	– –	–	–
Slices	1B, 1D, 2B, 2D, 3A, 3C	3A 210 mm 3B 0 mm	1B accumulation	1B normal	3B	2C	4D,E,F 110°	4D,E,F 110°
Quantity of angles [n]	563	16	21	9	16	11	24	15
Dominant shell axis	160–180°/ 340–360° **23.1 %**	160–180°/ 340–360° **68.8 %**	180–200°/ 000–020° **52.4 %**	220–240°/ 040–060° **33.3 %**	160–180°/ 340–360° **31.3 %**	160–180°/ 340–360° **36.4 %**	180–200°/ 000–020° **50.0 %**	geopetal axis 180–200°/ **29.4 %**
Dominant angle interval	160–200°/ 340–020° **45.2 %**	160–200°/ 340–020° **93.8 %**	160–200°/ 340–020° **81.0 %**	no dominant angle interval	160–200°/ 340–020° **43.9 %**	160–200°/ 340–020° **63.7 %**	160–200°/ 340–020° **70.8 %**	geopetal axis 340–360° **52.9 %**
Comments on axis angle	bimodal	weakly oblique, unimodal	weakly oblique, unimodal	polymodal	polymodal	weakly oblique, unimodal	weakly oblique, unimodal	shifted to ammonoid axes, polymodal
Dominant body chamber, up	160–180° **14.4 %**	160–180° **31.3 %**	000–020°, 160–180° both **14.3°**	000–020°, 40–60°, 140–160° all **14.3°**	160–180° **25.0 %**	000–020°, 140–160°, 160–180°, all **18.2°**	000–020° **20.8°**	–
Dominant body chamber, down	180–200° **10.1 %**	340–360° **37.5 %**	180–200° **38.1 %**	220–240°, 340–360° both **22.2 %**	180–200°, 340–360° **6.3 %**	340–360° **18.2 %**	180–200° **29.2 %**	–
Comments on body chamber angles	weakly oblique, unimodal	bimodal	bimodal	bimodal to polymodal	bimodal to polymodal	weakly oblique, unimodal	bimodal	–
Size classes and diameters								
Duantity of diameters [n]	563	16	21	9	15	11	21	–
Dominant size class [mm]	4.2–6.2 **26.6 %**	4.2–8.2 **37.6 %**	8.4–10.4 **38.1 %**	0.0–4.2 **66.6 %**	6.3–10.4 **40.0 %**	6.3–8.3 **45.5 %**	10.5–12.5 **23.8 %**	–
Dominant size range [mm]	2.2–10.2 **80.0 %**	4.2–12.2 **56.3 %**	2.1–10.4 **66.7 %**	0.0–6.2 **88.9 %**	4.2–16.7 **80.0 %**	4.2–10.4 **100 %**	2.1–12.5 **61.9 %**	–
Dispersal curve	unimodal, positively skewed	broad unimodal to bimodal	broad unimodal to bimodal	unimodal, positively skewed	bimodal	unimodal, positively skewed	broad bimodal	–
Mean size [mm]	7.2	12.9	9.9	3.5	10.7	6.9	12.1	–
Comment on size	small	larger	small	very small	larger	small	larger	–
Miniumum size [mm]	1.0	4.4	1.9	1.6	3.5	5.3	2.0	–
Maximum size [mm]	20.2	25.9	20.2	8.8	19.0	10.3	26.8	–
Size range [mm]	19.2	21.5	18.3	7.2	15.5	5.0	24.8	–

(e.g. blocks 1, 2) the aligned ammonoids are accumulated in a shell coquina on the top of laminated, peloidal 'silts'.

The body chambers are filled with the same matrix, which is formed by peloids from a shallower environment, representing the primary depositional area. The shells are densely packed, well sorted and in contact with numerous other shells. The densely packed accumulation layer marks an ammonoid packstone. Siphonal structures are preserved, hindering sediment to fill the phragmocones (see Olivero 2007), hence rapidly buried after death exhibiting the final, hollow 'particles' embedded in the peloidal layers. The matrix above and below this event layer differs distinctly as it consists of fine mud with only rare and smaller ammonoid specimens, deposited under 'normal' conditions. An additional block from AS IV (i.e. block 3) marks a 'normal' calm deposition at, or near the habitat of the ammonoids, appearing with rare, entire ammonoid shells with almost undisturbed and horizontal alignment (Fig. 9, Table 1). The shell axis in block AS IV — block 3 shows a clear picture with dominant intervals at 160–180°/340–360° with 75.0 % and even more expressed in the interval 160–200°/340–020° with 97.2 %.

The acme zone of the genus *Kasimlarceltites* ranges due to tectonics from 1.8 m at AS Ia to 16.5 m at KA II, and is intercalated by accumula-

tion event beds (Figs. 2, 3, 4, 7). On the basis of the geological time scale of Gradstein et al. (2012) a stratigraphical range from one third to one half of the *Austrotrachyceras austriacum* Zone can be assumed, which approximately equals a duration of 200 ky (at AS I, AS IV)–500 ky (at KA II) for the *Kasimlarceltites* abundance zones. This time span is calculated without consideration of any hiatus or time-averaging, which might occur. The overall quantity of more than 100 million ammonoid specimens is estimated by the data gained from numerous localities from Aşağıyaylabel and Karapınar (e.g. layer thickness, number of mass occurrence layers and specimens etc.) and the geographical distribution (over 10 km^2) of the *Kasimlarceltites* abundance zone. Single blocks from both localities (Aşağıyaylabel and Karapınar) with 15×15×8 cm contain up to 3500 specimens (Mayrhofer & Lukeneder in prep.).

The calculated mean angle of all combined sections and specimen axes (n 1696) in frontal view is almost horizontal with 172°/352° (Fig. 10) indicating a shallow orientation (low angle) of ammonoid shells throughout the various localities (Tables 1, 2, 3). Within the polyspecific KA II — block 4 an increased angle with 164°/344° was observed, as well as an increased number of steeper orientations in body chambers. In contrast the mean angle of shell axes in KA II — block 3 is shallow (low angle — almost planar) with 178°/358°. The measured angle is influenced by the ontogenetic stage and the morphological differences in whorl height. Adult specimens show an angle of 2° whereas juveniles appear with 3° owing to the different whorl expansion rates.

The same situation can be observed in the combined orthogonal data (Fig. 10, Table 3). The mean angle of all specimen axes (n 1696) in orthogonal view is 177°/357° (172°/352° frontal), depicting a very shallow orientation of ammonoid shells throughout the various localities. Anyhow, an increased angle of 15°/195° in KA II — block 4, where *Kasimlarceltites* occurs together with some specimens of *Sirenites*, was detected. As already observed in frontal view, the orthogonal data strengthen the contrasting picture with an almost horizontal, very shallow mean angle of shell axes in KA II — block 3 by 179°/359° (Fig. 10, Table 3). The lower accumulation layer in KA I — block 1a (Fig. 10) shows mean angles of 004°/184° whereas the 'normal' sedimentation part above (KA I — block 1n; Fig. 10) appears with an increased angle of 018°/198°.

Size groups in Kasimlarceltites

In general the ceratitid genus *Kasimlarceltites* Lukeneder & Lukeneder (2014) is a small sized, 1.0 to 3.3 cm, almost smooth ammonoid. The abundance of different ontogenetic stages within the occurring size classes (Fig. 10, Tables 2, 3) varies from locality to locality, even from layer to layer in the same locality. Densely spaced sutures at the phragmocone/body chamber boundary of some specimens mark the adult stage in numerous ammonoids. For more detailed description see Lukeneder & Lukeneder (2014, fig. 4–5). At different localities minimum and maximum range size values of *Kasimlarceltites* differs markedly (Fig. 10, Tables 2, 3).

Size ranges and dominant diameters (in mm) are given for all accumulation layers, in frontal and orthogonal direction for comparison of potential spatial alignments (Fig. 10, Tables 2, 3).

Aşağıyaylabel

Frontal (Fig. 10, Table 2)
AS Ia, AS IV
Orthogonal (Fig. 10, Table 3)
AS Ia, AS IV

Karapınar

Frontal (Fig. 10, Table 2)
KA I, KA II
Orthogonal (Fig. 10, Table 3)
KA I, KA II

The overall impression fixed by the data (i.e. angles and diameters) of all specimens measured (n 1696) in frontal views shows a unimodal positively skewed distribution of size classes. For better comparison of distribution, curve shapes and visualization of size classes, distribution curves were set to 100 % (Fig. 10). A clear dominance of small forms from 2.1–12.5 mm is evident (Fig. 10). The maximum size class appears at 4.2–6.2 mm. Maximal size classes from 25.2–29.3 mm are rare to absent in most localities. From the taxonomical work by Lukeneder & Lukeneder (2014) on prepared specimens from the same localities, a maximal diameter of *Kasimlarceltites* is known with 33 mm. The difference in maximal diameters of about 37 mm shows the uncertainty and imprecision in numerical measurements in slices and sections, since the majority of excavated ammonoids from the sections miss the aperture area and therefore fail to reflect the maximum size.

Specimens from AS Ia — block 4, AS Ia — block 3 and KA I — block 1 show their maximum size in frontal view with unimodal curves (positively skewed) at 2.1–10.4 mm. Somewhat shifted curves, increasing in mean size, are present in KA II — block 2 (bimodal) and KA II — block 3 with positively skewed, unimodal curves around a maximum of 4.2–14.6 mm. Exceptional, broad distribution curves occur in AS IV — block 3 with 2.1–23.0 mm and KA I — block 1 with 2.1–20.9 mm.

Analogously, the picture of all specimens measured (n 675) in orthogonal views show a unimodal positively skewed distribution of size classes. The abundance peak also lies within the class 4.2–6.2 mm as seen in the frontal view (Fig. 10). A clear dominance of small forms from 2.1–10.4 mm is established (Fig. 10). The maximum size class appears at 4.2–6.2 mm. Maximal size classes from 25.2–27.2 mm are rare to absent in some localities.

Specimens from AS Ia — blocks 1, 2, 3 and KA II — block 2 show the maximum size in frontal view with unimodal curves (positively skewed) at 2.1–10.4 mm. Somewhat shifted curves, increasing in mean size, with a slightly bimodal mode are present in AS IV — block 3 and KA I — block 1a (accumulation layer) with positively skewed curves around a maximum of 4.2–14.6 mm. Exceptional, broad distribution curves occur in KA II — block 3 with a wide range of 2.1–18.8 mm.

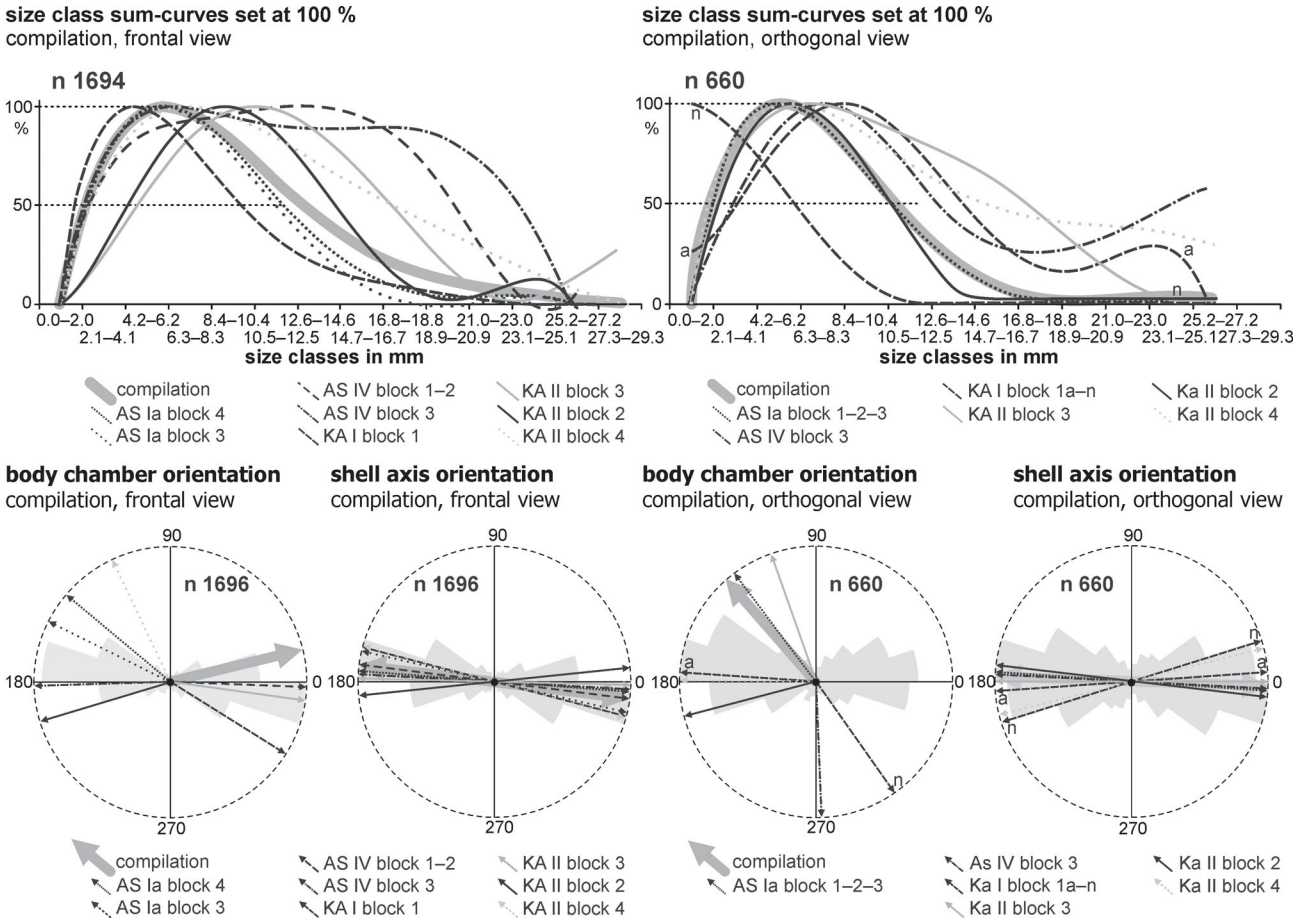

Fig. 10. Compilation of size classes, shell axes and body chamber orientations from *Kasimlarceltites* in frontal and orthogonal view of all measured blocks of Aşağıyaylabel (AS I, AS II, AS III, AS IV) and Karapınar (KA I, KA II), Kasımlar Formation, *Kasimlarceltites* acme zone, Lower Carnian, Upper Triassic. See text for description and details.

Variation in diameters and size classes, as reported above for angles, is also present within single layers, as seen in KA I — block 1 (a — accumulation, n — normal). The lower accumulation layer (KA I — block 1a; Fig. 10, Tables 2, 3) shows an abundance of the mean size class 4.2–12.6 mm, whereas the normal sedimentation part above (KA I — block 1n) appears with a decreased diameter class of 0.0–6.2 mm. Both distribution curves are positively skewed but KA I — block 1a shows weak bimodal distribution. Hence the latter ammonoid assemblage comprises juvenile and adult specimens. While juvenile specimens are compressed in shape, adult specimens are much more depressed. This might be interpreted as mating community, environmental forcing or transport mechanism (e.g. current or drift selection of different size or morphology classes).

Discussion

The Kasimlarceltites mass occurrence as an abundance zone

The trigger mechanisms and possible processes, which cause the abundance and accumulation of ammonoids and the formation of such widespread ammonoid mass occurrences or 'event' layers, are discussed. Current induced alignment, winnowing and earth quakes or storm events (Aigner 1985; Brett & Baird 1986; Seilacher & Aigner 1991; Hips 1998; Radley & Barker 1998; Storms 2001; Pérez-Lopéz & Pérez-Valera 2012) are discussed as trigger factors for such gravity forced 'event beds'. The described examples are thus autocyclic (Einsele et al. 1991b), formed by nonperiodic mass flows and/or turbidites endemic to the tectonic setting (Bouma et al. 1982; Cook et al. 1982; Howell & Normark 1982; Tucker & Wright 1990; Potter et al. 2005; Hornung 2008). Final deposition took place on tectonically unstable slope areas, shown by the presence of frequent neptunian dykes (see Flügel 2004; Črne et al. 2007) within the *Kasimlarceltites* acme zone.

In the majority of such fossil accumulation beds, several reasons amplify the primary signal (Kidwell 1986; Kidwell et al. 1986). Pérez-Lopéz & Pérez-Valera (2012) presented a tripartite model for storm influenced beds and near platform carbonate environments with the pot/gutter casts, the tempestite beds and the storm winnowed deposits. According to Aigner (1985) storm processes can be distinguished in three distinct physical categories with barometric effects, wind effects, and wave effects. The causes and features of such rapidly deposited 'event' sediments are extensively reviewed by

Einsele & Seilacher (1982) and Einsele et al. (1991a), and the depositional environment of sandy turbidites and other mass flows deposits are summarized by Einsele (1991).

As noted by Aigner (1985), storm-generated tempestites show a clear gradation with fine sediments that is extremely subtle or lacking in distal tempestite fronts (difficult to separate from distal turbidites), which is not seen in the Carnian layers at Aşağıyaylabel and Karapınar. Specifically, he noted that proximal storm-event layers contain more mixed faunas, with allochthonous specimens, in contrast to distal layers, where autochthonous and parautochthonous assemblages predominate, having been reworked *in-situ* (see also Golebiowski 1991).

Progressing gravity, debris flows show typical transition to turbidity currents, due to changes in different transportation phases when variable degrees of debris dilution occur. Therefore the transportation of debris might indicate net reworking (pers. comm. Olóriz 2014).

The dynamic history and the influence of sediment transport to that area during the Carnian can also be traced by the frequent Cipit boulders (directly above the *Kasimlarceltites* acme zone), derived from the shallow-platform edge and transported by gravity down across the slope, as well as by the frequently silty, turbidite layers in the Kasımlar shales in the Tuvalian.

Geochemical and geophysical data (Lukeneder et al. in prep.) will confirm or contradict the idea of drastic changes in ecological factors (e.g. anoxic events, methane eruptions, for toxic events see also Noe-Nygaard et al. 1987) during the sedimentation of the *Kasimlarceltites* acme zone. Such ecological factors can act as trigger mechanisms for potentially catastrophic ammonoid mass mortality of the ammonoid deposits from Turkey. Such traces are not observed in the redeposited layers (episodic deposits in Brett & Baird 1986) and in the 'normal', background sedimentation beds (='host' beds) where *Kasimlarceltites* rarely occurs. In contrast to this, Adamíkova et al. (1983) discussed mass natality as a possible trigger for a lower Barremian (Cretaceous) mass occurrence of ammonoids (Adamíkova et al. 1983).

The presence of ammonoid abundance zones ('ammonoid-beds'; characterized by abundance or mass-occurrence of ammonoids) seems to be related to sea-level rises or falls (Kidwell 1988, 1991a,b, 1993a,b; Martin 1999; Lukeneder 2001, 2003b). Most probably ammonoid mass occurrences reflect transgressive phases (see also Hoedemaeker 1994; Aguirre-Urreta & Rawson 1998, 1999). Anyhow, Fernández-López et al. (2002) argued that ammonoid mass occurrences deposited within shallow water environments reflect regressive phases, whilst ammonoid mass occurrences deposited within deeper water environments reflect transgressive trends (Fernández-López et al. 2002). The observation of different preservational features (e.g. sedimentary infilling, encrustation, abrasion, bioerosion, reorientation and dispersal) might hint to the right interpretation (a shallow or deeper-water environment — Fernández-López et al. 2002).

Biostratinomy and taphonomy

The nearly entire (>95 %) well preserved ammonoid specimens of the lower Upper Triassic (Carnian) of the Kasımlar Formation, suggest no-to-moderate, non-destructive transport mechanisms and therefore favour a more autochthonous to parautochthonous nature of the specimens. Judging from internal structures of the limestone beds and the alignment of the fossil content (Potter & Pettijohn 1977), water saturated gravity flows (=liquified flows — Mulder & Alexander 2001; SEPM 2014) are induced at a medial position between a proximal (near-source) and a distal depositional development (see Aigner 1985). Hence, moderate transportation of at least some intraclasts, plasticlasts and bioclasts such as gastropods and in parts ammonoids, is presumed.

The fragmentation (e.g. broken body chamber) of less than 5 % of the ammonoids provides evidence for no, gentle or very weak post mortem transport, without breakage on the sea floor through current effects, and/or consequences of predation (Lukeneder 2004a,b). Anyway, the tiny shells (max. 33 mm) of *Kasimlarceltites* were probably resistant against breakage by impact of shells with other bioclasts transported by the currents. Ruptures reflecting post mortem histories, caused by current-induced transport before embedding, are absent. It may also reflect the enhanced stability of ammonoid shells with smaller size, more 'spheroidal' shape and suggests that involute morphologies are more resistant to damage compared to other ammonoid shell morphologies (e.g. broken body chamber of *Simonyceras*; specimen figured on Fig. 11A in Lukeneder & Lukeneder 2014). Furthermore, buccal masses with preserved beak apparatus (e.g. aptychi like jaws) are completely missing in the Turkish material, hinting at more parautochthonous than autochthonous depositional conditions.

Accumulated small ammonoids (i.e. *Kasimlarceltites*) of all ontogenetic stages (e.g. ammonitellae, juveniles to adults) and shell fragments in body chambers of adjacent large ammonoids, in combination with cephalopod alignment in several single layers (e.g. AS Ia — beds 4, 6; AS IV — bed 8; KA I — beds 10, 12; KA II — beds 2, 11, 122; KA III — bed 8) also suggest transport-effects on deposition (e.g. mass flow, bottom currents, winnowing — Potter & Pettijohn 1977; Flügel 2004; Potter et al. 2005; Fernández-López 2007; Nichols 2009). The accumulation of the shells which show almost horizontal alignment (Figs. 8, 9, 10) in thin and distinct layers, is probably due to episodes of reworking and current-induced removal of sediment (i.e. winnowing). Horizontally aligned specimens were most probably secondarily re-orientated and aligned during a first gravity flow sedimentation phase.

The absence of any erosional feature (i.e. mechanical- or bio-erosion; see Fernández-López 2007) or encrustation on any side of the ammonoids suggest calm environments with relatively fast burial processes. The shell transport took place during single events or phases of slow gravity sediment flows, as is reflected by the occurrence in several separated ammonoid layers up to 10 cm in thickness (Figs. 3, 4, 5, 7).

The 'normal' occurrence range, with rare specimens of *Kasimlarceltites,* clearly shows the inhabitation of that paleogeographical area during the Carnian (Late Triassic) over a hundred thousand years (Lukeneder & Lukeneder 2014; for numerical age see Gradstein et al. 2012). In contrast, accumulation in masses occurs only within single event beds,

caused by huge storms or tectonically induced earthquakes (=seismic activity in Einsele 1991; see slope failures in Potter et al. 2005).

Mixed assemblages are defined in Lukeneder (2004a,b) as comprising allochthonous elements (e.g. gastropods, sponges, corals) transported from the shallower shelf to upper slope and autochthonous benthic and parautochthonous pelagic elements (e.g. ceratitid ammonoid *Kasimlarceltites*) from deeper marine environments. See also the discussions by Olóriz & Villaseñor (2010) on post-mortem and possible biostratinomic mixing of ecologically age-separated populations. Assuming an analogous situation for the Aşağıyaylabel sections as for the Karapınar sections, this would mean that the presence of undamaged macroconchs accompanied by intact microconchs within the same bed points to a similar derivation of the ammonoids from the same source, in this case the pelagic fauna of the water column above, without assuming any depth. This points to a huge problem in the understanding of ammonoids life and habitats. The question, if ammonoids in general, and *Kasimlarceltites* or *Sirenites* from Turkey in detail, were planktonic drifters, nektic swimmers or nektobenthic swimmers is beyond the field of the study here. Nonetheless, the answer to this question would make a serious difference to the study of biostratinomic features in chambered cephalopods, both fossil (e.g. ammonoids, nautiloids) and recent (e.g. *Nautilus*, *Spirula*).

The *post mortem* history, hence the subsequently complicated drifting mechanisms (i.e. waterlogging and sinking versus surfacing and floating; see Seilacher 1968; Olivero 2007) in ammonoid shells depends mostly on the water depth and hydrostatic pressure (Maeda & Seilacher 1996) when the animal dies. This interpretation is contrasted to the occurrence of some specimens showing different sediment-infillings of the body chambers as compared to the surrounding and embedding finer limestone. Reasons for these differences in sediment infilling reflect the difference in sediment and shell transportation history. Specimens filled with coarser material (i.e. shallower water relicts) are redeposited from shallower areas. Shells are preserved without fragmentation (i.e. body chamber present), mostly with almost similar alignment and rare infilling of phragmocones by sediment (see Olivero 2007). Observed geopetal structures, aligned in almost identical directions, within the accumulated ammonoids give evidence for a fast burial history of almost the entire contingent of ammonoids. Ammonoid specimens shown by Olivero (2007) from the Santonian–Lower Campanian mass flow deposits of Antarctica also exhibit preserved siphuncle tubes preventing the infill of phragmocones with sediment.

The cephalopods of the Aşağıyaylabel and Karapınar sections thus constitute a mixed autochthonous/parautochthonous/allochthonous (Martin 1999) fauna. This effect is enhanced by the fact that gravity currents, submarine mass-flows (mud supported and water saturated) may already contain a mixed shelf and slope assemblage by picking up bioclasts from different bathymetric zones along their way (Einsele & Seilacher 1991). The Carnian mixed assemblages comprise a considerable amount of bivalves, gastropods, sponges and corals from shallower environments from a nearby located platform or upper ramp (Lukeneder et al. 2012; see Eberli 1991). The term 'mixed' assemblage is used in the sense of Kidwell & Bosence (1991). The latter authors described a mixed assemblage as the addition of shells of one assemblage to the members of another assemblage. For classification and reviews on taphonomic processes of marine shelly faunas see also Norris (1986), Kidwell et al. (1986), Brett & Seilacher (1991), Kidwell (1991a,b), Kidwell & Bosence (1991), and Speyer & Brett (1991).

Ammonoid shell alignment

The ammonoid shell orientation (i.e. rose diagrams of shell axes, body chamber orientation; Figs. 9, 10, 11) within the accumulation layers was measured to gain information on the prevailing conditions and mechanisms (e.g. bottom water currents, debris flows, turbidites, storms etc.; Goldring 1991) at the time of deposition (Early Carnian, *Austrotrachyceras austriacum* Zone).

A more detailed picture of the three-dimensional alignment of specimens from AS I–block 1 (i.e. 150×45×140 mm block, 70 slices with 2 mm distance) is presented in Lukeneder et al. (2014). Lukeneder et al. (2014) show that the internal, dominant orientation of specimens in fossil mass occurrences can be exploited as a useful source of information about the flow type and direction determining the precise conditions for their transportation and accumulation. A series of studies, using different kind of fossils, especially those with elongated shape (e.g. elongated gastropods), deal with their orientation and the subsequent reconstruction of the depositional conditions (e.g. paleocurrents, transport mechanisms). However, disk-shaped fossils like planispiral cephalopods or gastropods were used, up to now, with caution for interpreting paleocurrents. Moreover, most studies just deal with the topmost surface of such mass occurrences, due to its easier accessibility. Within Lukeneder et al. (2014) the exact spatial shell orientation was determined for a sample of 675 ammonoids, and the statistical orientation analysed with a NW/SE-orientation. The study of Lukeneder et al. (2014) from the Aşağıyaylabel mass occurrence combines classical orientation analysis with modern 3D-visualization techniques, and establishes a novel spatial orientation analysing method, which can be adapted to any kind of abundant identifiable object. Such a spatial alignment with imbrication in a gravity flow was detected by Hladil et al. (1996) for Lower Devonian tentaculite shells from the Czech Republic. There, the analysed fossils show a similar oblique orientation (i.e. upward and downward) due to gravity transport (Hladil et al. 1996), caused by a rapid consolidation of the host sediment. It should be noted that the natural, post mortem orientation angle of a particular ammonoid shell (i.e. *Kasimlarceltites*) after sinking onto the sea floor, is almost horizontal with approximately 2–3° (Fig. 8), depending on the ontogenetic stage. This phenomenon is caused by the maximal whorl breath at the body chamber near the aperture. The horizontal shell orientation dominates over oblique alignment in layers formed during undisturbed backround sedimentation.

The Triassic assemblages differ significantly from a Middle Devonian example of nautiloid mass occurrences (=con-

centrates in Soja et al. 1996), which was interpreted as being a combination of mass spawning and mass mortality events (biological process; see Lukeneder, in print) with storm-related accumulations (physical process). In contrast to the Triassic accumulation layers from Turkey, the densely packed Devonian cephalopod mass occurrence (i.e. nautiloid grainstone) shows no orientation, alignment or imbrication of the shells (Soja et al. 1996). *Goniatites* beds from Upper Devonian of Poland (Niechwedowicz & Trammer 2007) were described as post mortem shell accumulation, not transported very far, deposited within the habitat realm and interpreted as the result of condensation, which has often been noted for cephalopod limestones. Niechwedowicz & Trammer (2007) interpreted the shell alignment due to wave or current transport in shallower environments.

At least some of the abundant ammonoid specimens seem to have been redeposited from shallower shelf regions into a slope environment. Similar occurrences were reported from low density gravity flows (e.g. slump deposits and turbidites) from Lower Triassic redeposited ammonoid accumulations of East Russia (Maeda & Shigeta 2009). The authors note sporadically intercalated ammonoid beds (with nearly horizontal alignment of ammonoid shells) within otherwise 'normal' mudstone sedimentation. Maeda & Shigeta (2009) identified an allochthonous source (i.e. primary shelf edge biotope) for ammonoids deposited and transported in such fossiliferous, turbidite layers. Taxonomical related findings of celtitids were presented by Manfrin et al. (2005) from adjacent basinal series, surrounding the Middle Triassic Latemar Platform (N Italy). The faunas from these ammonoid layers were interpreted by Manfrin et al. (2005) as storm deposits, due to the mixture of pelagic and platform derived fossils and the partly perpendicular (= non-equilibrium in Manfrin et al. 2005) alignment of ammonoids within the coquinas. It is evident that such layers consist of transported, mixed faunal elements (i.e. pelagic ammonoids and benthic gastropods — Manfrin et al. 2005), deposited by distinct and short events. This is almost identical to the assemblages found at Aşağıyaylabel, but with the remarkable difference of chaotic shell-alignment, enhanced shell-fracturing and variation of sedimentological features.

Mass flow transport is evident from the orientation of shells within the layers (Middleton & Hampton 1973, 1976; Brown & Loucks 1993; Potter et al. 2005; Nichols 2009), not only at the top of beds as is the case when water current causes mass occurrence or turbidite accumulation. A somehow mixed or transitional mechanism of debris flow (i.e. laminar flow) and turbidity current (i.e. turbulent flow) deposition is assumed for floatstones of AS Ia and AS II. A low density, less concentrated and water saturated debris flow (= liquefied debris flow) with transitional features into a turbidite transport (pers. comm. Michael Wagreich 2013; see Lowe 1982; Einsele 1991; Hladil et al. 1996; Mulder & Alexander 2001; Olivero 2007) is highly presumable. A horizontal or at least low-angle deposition of imbricated shells is caused by low-density transports (Hladil et al. 1996). A positive enhancement of an existing inclination can be forced by slipping or sliding processes of the not consolidated sediment layers, down the slope or ramp.

The mostly erosive base of the accumulation layers, furthermore undulated with fragmented ammonoid shells, reflects sudden and punctual reworking phases at the base of the sediment flow to some extent (see Sepkoski et al. 1991).

The majority of the accumulation layers (AS I — beds 4, 6; most beds at KA I, KA II) were formed by water saturated debris flow deposition which caused the alignment of the biological particles (i.e. ammonoid shells) within the sediment. A contrasting exception can be observed in section AS IV (e.g. bed 8; Figs. 10, 11, Tables 1, 2, 3) and KA II within the blocks 1 and 4. In blocks 1 and 2 (corresponding to the same layer) in AS IV and KA II (e.g. blocks 1, 2) a clear short-term turbidite transport took place. Ammonoid shells seem to float on the peloidal-silt level, most probably due to hydrodynamic sorting. Hence, low density, empty ammonoid shells (1.1–1.2 g/cm^3 — Maeda 1999; Maeda & Shigeta 2009), subsequently filled by calcite, remain suspended in the water column during or shortly after the transport event.

All of the distinct ammonoid event layers represent only episodic (i.e. formed during days to weeks), punctual thin horizons (see Brandner et al. 2012) which interrupt the 'normal' background sedimentation phase, consisting of limestone beds with only rare occurrences of ammonoids (e.g. *Kasimlarceltites*, *Klipsteinia*, *Sirenites*). Brett & Baird (1986) distinguished two kind of deposition, characterized by the mode of sedimentation rate with the long-lasting background deposition (1–10 cm/10^3 yr) and the punctual episodic sedimentation (1–50 cm/10^{-2} yr).

The almost horizontal alignment of the shells from the ammonoid-rich horizons reflects the normal long-term sedimentation and no-to-weak transport of shells before embedding. The observed angle is similar to angles detected when single specimens are lain on a horizontal ground (Fig. 8). Contrastingly, the increased angle in the polyspecific KA II — block 4 with 164°/344° (frontal data) resp. 15°/195° (orthogonal data) is interpreted as caused by a more turbulent transport and the mixture with specimens of the bigger *Sirenites* (strong ribs and spines), on which *Kasimlarceltites* (almost smooth) specimens often 'lean'. The increased obliqueness in axes is also caused by the increased number of steeper orientations in body chambers with a mean direction of 111° in KA II — block 4 (Fig. 10).

The increased angle seems to reflect bioturbation and secondary dislocation of the small objects (i.e. 0.5–8.0 mm). Such small sized skeletal objects are easily orientated by common depositional processes (e.g. bottom currents, turbidites, storms, mass flows) but not obliged to be aligned related to their shell axes, owing to the almost globular morphology of small objects.

A more indistinct and imprecise picture is seen when interpreting the body chamber orientation in both, frontal and orthogonal two-dimensional slices (Fig. 10, Tables 2, 3). As the body chamber length in *Kasimlarceltites* varies from three-fourths to an entire whorl (i.e. mesodome to longidome; see Westermann 1996), measurements and data can only show the direction of the biggest part of the outer whorl, not assuming to show the definite, final apertural direction. This problem should be solved with 3D sectioning and reconstruction (Lukeneder et al. 2014). Hence the data

show unimodal (only one direction of body chambers) to bimodal (two opposite directions) distribution roses (Fig. 10). As shown above, the data on axes orientations, hence the transport induced directions and alignments are more reliable within our two-dimensional based work.

Size groups in Kasimlarceltites

The intraspecific variation of size classes and the difference within layers and localities is the expression of either different sources (i.e. environments, depth range) of the transported sediment (i.e. including ammonoids shells), or the result of sexual (i.e. females = macroconchs — M, males = microconchs — m) or ontogenetic (i.e. ammonitellae, juveniles and adults) separation of ammonoids habitats during life.

The difference in abundance and resulting distribution curves from frontal and orthogonal size classes in several blocks of different localities, once again strengthens the concept of an alignment of ammonoid shells after intense and detectable transport. This important issue can be noticed in KA II — block 2 with frontal values of 8.4–10.4 mm versus smaller orthogonal values between 4.2–6.2 mm, KA I — block 1 smaller frontal values (4.2–6.2 mm) versus orthogonal values (8.4–10.4 mm), and AS IV — block 3 with a frontal wide range (6.3–18.8 mm) versus a narrow orthogonal range of 6.3–8.3 mm and a second peak at 25.2–27.2 mm. Frontal and orthogonal size class distribution is almost identical in AS Ia — blocks 1, 2, 3 (Fig. 10).

Conclusions

The Upper Triassic macrofauna of Aşağıyaylabel and Karapınar (Taurus Mountains, Turkey) is represented especially by ammonoids (i.e. ceratitids) and bivalves (i.e. halobiids). The whole section yielded over 2300 ammonoids, extracted and prepared as well as embedded in blocks and sections. The fauna can be assigned to the Lower Carnian *Austrotrachyceras austriacum* Zone (Lukeneder & Lukeneder 2014) and contains ammonoids of all ontogenetic stages, from ammonitallae to adults (for more detail see Lukeneder & Lukeneder 2014).

The invertebrate fauna (e.g. ammonoids, bivalves, gastropods, sponges, corals) is accumulated in isolated and distinct single-event layers. The cephalopod shells are aligned and concentrated in particular levels and some show, to some extent, current-induced orientation. Alignment of shells into diverse orientations suggests mass flow currents or other turbulent bottom-water currents.

The ammonoid fauna at Aşağıyaylabel and Karapınar were deposited together with sediments formed by gravity induced flows and turbidites under the influence of winnowing and bottom currents. The sediments were partly reworked and transported in suspension for some distance, from shallower areas at the platform edge to the upper slope onto the deeper parts of the slope and basin. The sediments were initially deposited on the platform shelf close to the slope edge (shelf break area), which is also near the final embedding place of the ammonoid remains. In this area, unstable marine sediment accumulations create the prerequisite conditions for remobilization by gravity flows and/or turbidity currents (Einsele 1991; Potter et al. 2005). Those flows and currents then built up the floatstones and packstones comprising the ammonoid mass occurrences. The final deposition of the floatstones to packstones from Aşağıyaylabel and Karapınar took place on tectonically unstable slope areas during conditions of relatively high sedimentation rates. Successions with abundant or accumulated ammonoid-layers are widespread over a 15 km^2 area.

Debris flows and turbidity current, or a combination of both, were triggered either by storm wave activity or by forcing other physical events such as earthquakes, tsunamis and less probably sediment overloading, which led to the formation of event beds and ammonoid accumulation layers on the upper slope to basin of the Carnian (*Austrotrachyceras austriacum* Zone) from the Taurus Mountains. The ammonoid accumulation layers (and therefore the lower part of the Kasımlar Formation) are almost monospecific, dominated by the ceratitid genus *Kasimlarceltites* with up to 99.9 %. The thickness of the *Kasimlarceltites* acme zone ranges from 1.8 m at Aşağıyaylabel (section AS I) and 16.5 m at Karapınar II (section KA II). The position, and hence the exact geographical cardinal direction of the source area, is unknown.

The orientation measurements (e.g. angles of axes and body chambers) of the ammonoids also point to origination by water-saturated, liquefied debris flows, resulting in biogenic floatstones or packstones (i.e. matrix supported and ammonoid shell supported; see Flügel 1978, 2004). The twofold picture clearly points to various transport mechanisms, hence a change of source areas or transport history during the Julian–Tuvalian in Carnian times (Late Triassic). An increasing water depth, either due to a sea level rise or a tectonic drop of the carbonate platform is also evident for that Anatolian area, clearly detectable in the sedimentological and paleontological record. Subsequently, current systems changed during that time of paleo-oceanographic modification and restructuring, resulting in unstable conditions and thus redeposited accumulation layers.

The *Kasimlarceltites* event layers are intercalated with 'normal' sedimentation beds, which are represented by wackestones with only rare, floating *Kasimlarceltites* specimens. Small ammonoids (i.e. juvenile *Kasimlarceltites*) and shell fragments in the body chambers of somewhat larger ammonoids also support the assumed effect of agglomeration and comminution by dense sediment flows with a laminar internal flow. The accumulation of ammonoid layers indicates either on-site deposition at short, favourable 'time-intervals', or reworked accumulation-layers after gravity flow transport (slow debris flow). Most ammonoid specimens are not fragmented and do not show bioerosion (i.e. boring, encrustation). This suggests a short transport history of the sediment masses and rapid incorporated shells (e.g. ammonoids, bivalves, gastropods) as well as relatively fast burial. Moreover, because most body chambers of the ammonoid specimens are filled with debris, they were already dead at the time when they were transported. These are thus true, redeposited accumulations, and their initial accumula-

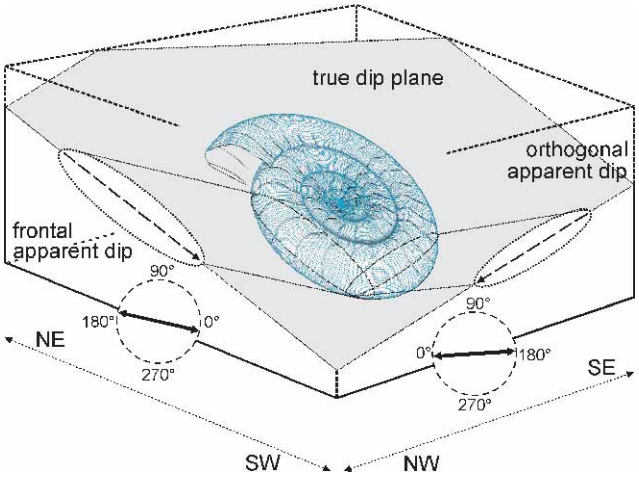

Fig. 11. Calculation scheme for true dip direction in ammonoid shells from Aşağıyaylabel (AS I, AS I — blocks 1, 2, 3, 4). True dip direction of the ammonoid shell 'plane' needs two different (frontal and orthogonal) apparent dip measurements of ammonoid shell axes. For more details on this method and three dimensional calculations see Lukeneder et al. (2014).

tion in shallow water must have also been characterized by fairly rapid burial, to avoid postmortem bioerosion. The presence of ammonoids bearing intraclasts (i.e. different colour due to different source areas), of sponges associated with corals and gastropods, of slightly dislocated shell angles in ammonoids, of dislocated geopetal structures (i.e. in ammonoid shells) and in cases of a cover of broken ammonoid shells and bivalve coquinas (Kidwell 1991a,b) signify a turbulent transport and redeposition of sediments and fossils.

The assemblages within the described accumulation layers depict an indefinite mixture of autochthonous (=indigenous in Kidwell 1991b), parauthochthonous, and allochthonous (=exotic in Kidwell 1991b) sedimentological and biogenic elements. Concentrations of ammonoid shells are mainly based on primary biogenic (sensu Kidwell et al. 1986) and sedimentological concentration mechanisms (see Kidwell et al. 1986; Meldahl 1993). The combination of both (biogenic and sedimentological skeletal concentrations) suggest inner shelf and inner ramp environments (Kidwell et al. 1986).

The enormous quantity of ammonoid shells in these thin beds also suggests a possible gregarious life style of the ceratitid *Kasimlarceltites*, at least during times of mating and spawning (see also Soja et al. 1996; Lukeneder, in print). Buccal masses with preserved beak apparatus (e.g. aptychi like jaws) are completely missing in the Turkish material. Isolation took place, either through transport, due to different behaviour within the water column, or through current-induced grain differentiation during accumulation. The latter scenario leads to different, and unknown, places of deposition for these two cephalopod elements of the same animal.

A highly variable sea floor morphology is induced by the lithological and sedimentological deviations within the adjacent sections. Bottom physiography produced different accumulation models and ammonoid shell bed types.

This leads consequently to the question of the time during which *Kasimlarceltites* dominated the fauna in this Late Triassic (i.e. Carnian — Julian 2) area. A stratigraphical range (Gradstein et al. 2012) from one third to one half of the *Austrotrachyceras austriacum* Zone (approximately 200 ky at AS I and AS IV — 500 ky at KA II) is calculated for the *Kasimlarceltites* acme zone, not considering any hiati or time averaging, which might have occurred. A possible geographical differentiation into habitats from sexual dimorphic pairs (i.e. females, males and juveniles), and hence the original water depths inhabited by different size and morphogroups, bears the potential to change the picture of the formation mechanisms and habitats in ceratitid ammonoids and to produce such mass occurrences or event beds in particular. The obtained information encourages future research focused on the preservation history and processes causing ammonoid accumulations.

Acknowledgments: This study benefited from Grants from the Austrian Science Fund (FWF) within the Project P 22109-B17. The authors highly appreciate the help and support from the General Directorate of Mineral Research and Exploration (MTA, Turkey) and are thankful for the digging permission within the investigated area. Special thanks go to Yeşim Islamoğlu (MTA, Ankara) for organizing and guiding two field trips. The authors thank Leopold Krystyn and Andreas Gindl (both University of Vienna), Mathias Harzhauser and Franz Topka (both Natural History Museum Vienna) and Philipp Strauss (Austrian Oil Exploration Company OMV, Vienna), who provided material from previous field trips. Simon Schneider (CASP, Cambridge, United Kingdom) and Thomas Hofmann (Geological Survey of Austria, Vienna) are acknowledged for their support in collecting literature. We thank Simon Schneider (CASP, Cambridge, United Kingdom) for explanations of some details concerning the new established method. Photographs of ammonoid specimens were taken by Alice Schumacher (Natural History Museum Vienna). We kindly acknowledge Susan Kidwell (University of Chicago), Federico Olóriz (Universidad de Granada) as well as Jozef Michalík (Slovak Academy of Science) for their comments, which greatly improved the quality of this manuscript. We are grateful to Michael Wagreich (University Vienna, Vienna) for discussions and helpful comments. We, the authors, dedicate the paper to Eva Chorvátová (Bratislava) who passed away much too early in 2014. She supervised the first steps of our submission to Geologica Carpathica.

References

Adamíkova G., Michalík J. & Vašíček Z. 1983: Composition and ecology of the "Pseudothurmannia-Fauna", Lower Barremian of the Krížna-Nappe in the Strážovské Vrchy Mts. *Geol. Carpathica* 34, 5, 591–615.

Aguirre-Urreta M.B. & Rawson P.F. 1998: The early Cretaceous (Valanginian) ammonite *Chacantuceras* gen. nov. — a link between the Neuquén and Austral basins. *Rev. Asoc. Geol. Argentina* 53, 354–364.

Aguirre-Urreta M.B. & Rawson P.F. 1999: Lower Cretaceous ammonites from the Neuquén Basin, Argentina: *Viluceras*, a new

Valanginian subgenus of *Olcostephanus*. *Cretaceous Research* 20, 343–357.

Aigner T. 1982a: Calcareous tempestites: storm-dominated stratification in Upper Muschelkalk Limestones (Middle Trias, SW-Germany). In: Einsele G. & Seilacher A. (Eds.): Cyclic and event and stratification. *Springer-Verlag*, Berlin–Heidelberg, 181–198.

Aigner T. 1982b: Proximiality trends in modern storm sands from the Helgoland Bight (North Sea) and their implications for basin analysis. *Senckenberg. Marit.* 14, 183–215.

Aigner T. 1985: Storms depositional systems. In: Friedman G.M., Neugebauer H.J. & Seilacher A. (Eds.): Lecture notes in Earth Sciences. 3. *Springer-Verlag*, Berlin–Heidelberg, 1–174.

Allison P.A. & Briggs D.E.G. (Eds.) 1991: Taphonomy. Releasing the data locked in the fossil record. Topics in geobiology. 9. *Plenum Press*, New York–London, 1–560.

Andrews T. & Robertson A. 2002: The Beysehir-Hoyran-Hadim nappes: genesis and emplacement of Mesozoic marginal and oceanic units of the northern Neotethys in southern Turkey. *J. Geol. Soc. London* 159, 529–543.

Bottjer D.J., Campbell K.A., Schubert J.K. & Droser M.L. 1995: Palaeoecological models, non-uniformitarism, and tracking the changing ecology of the past. In: Bosence D.W.J. & Allison P.A. (Eds.): Marine palaeoenvironmental analysis from fossils. *Geol. Soc. London, Spec. Publ.* 83, 7–26.

Bouma A.H., Berryhill H.L., Knebel H.J. & Brenner R.L. 1982: Continental shelf. In: Scholle P.A. & Spearing D. (Eds.): Sandstone depositional environments. *Amer. Assoc. Petrol. Geol., Mem.* 31, 281–327.

Brandner R., Horacek M. & Keim L. 2012: Permian-Triassic boundary and Lower Triassic in the Dolomites, southern Alps (Italy). *J. Alp. Geol.* 54, 379–404.

Brett C.E. & Baird G.C. 1986: Comparative taphonomy: a key to palaeoenvironmental interpretation based on fossil preservation. *Palaios* 1, 207–227.

Brett C.E. & Seilacher A. 1991: Fossil Lagerstätten: a taphonomic consequence of event sedimentation. In: Einsele G., Ricken W. & Seilacher A. (Eds.): Cycles and events in stratigraphy. *Springer-Verlag*, Berlin–Heidelberg, 283–297.

Brown A.A. & Loucks R.G. 1993: Toe of slope. In: Bebout D.G. & Kerans C. (Eds.): Guide to the Permian reef geology trail, McKittrick Canyon, Guadalupe Mountains National Park, West Texas. *The University of Texas at Austin*, *Bureau of Economic Geology Guidebook* 26, 5–13.

Carrillat A. & Martini R. 2009: Palaeoenvironmental reconstruction of the Mufara Formation (Upper Triassic, Sicily): High resolution sedimentology, biostratigraphy and sea-level changes. *Palaeogeogr. Palaeoclimatol. Palaeoecol.* 283, 60–76.

Chuanmao L., Friedman G.M. & Zhaochang Z. 1993: Carbonate storm deposits (tempestites) of Middle to Upper Carnian age in the Helan Mountains, northwest China. *Carbonate Evaporite* 8, 181–190.

Cook H.E., Field M.E. & Gardner J.V. 1982: Characteristics of sediments on modern and ancient continental slopes. In: Scholle P.A. & Spearing D. (Eds.): Sandstone depositional environments. *Amer. Assoc. Petrol. Geol., Mem.* 31, 329–364.

Črne A.E., Šmuc A. & Skaberne D. 2007: Jurassic neptunian dikes at Mt Mangart (Julian Alps, NW Slovenia). *Facies* 53, 249–265.

Dercourt J., Ricou L.E. & Vrielynck B. 1993: Atlas Tethys palaeoenvironmental maps. *Gaulthier-Villars*, Paris, 1–307.

Dercourt J., Gaetani M., Vrielynck B., Barrier E., Biju-Duval B., Brunet M.F., Cadet J.P., Crasquin S. & Sandulescu M. (Eds.) 2000: Atlas Peri-Tethys-Palaeogeographical maps. *Commission of the Geological Map of the World*, Paris, 1–269.

Deynoux M., Çinar A., Monod O., Karabiyikoglu M. & Manatschal Tuzcu S. 2005: Facies architecture and depositional evolution of alluvial fan to fan-delta complexes in the tectonically active Miocene Köprüçayc Basin, Isparta Angle, Turkey. *Sed. Geol.* 173, 315–343.

Dumont J.F. 1976: Etudes géologiques dans les Taurides Occidentales: Les formations paléozoiques et mésozoiques de la coupole de Karacahisar (Province d'Isparta, Turquie). *Dissertation, University of South Paris*, 213.

Dumont J.F. & Kerey E. 1975: The Kırkavak Fault. [Kırkavak Fayı.] *Tür. Jeol. Kurumu. Bül.* 18, 59–62.

Eberli G.P. 1991: Calcareous turbidites and their relationship to sea-level fluctuations and tectonism. In: Einsele G., Ricken W. & Seilacher A. (Eds.): Cycles and events in stratigraphy. *Springer-Verlag*, Berlin–Heidelberg, 341–359.

Einsele G. 1991: Submarine mass flow deposits and turbidites. In: Einsele G., Ricken W. & Seilacher A. (Eds.): Cycles and events in stratigraphy. *Springer-Verlag*, Berlin–Heidelberg, 313–339.

Einsele G. & Seilacher A. (Eds.) 1982: Cyclic and event and stratification. *Springer-Verlag*, Berlin–Heidelberg, 1–536.

Einsele G. & Seilacher A. 1991: Distinction of tempestites and Turbidites. In: Einsele G., Ricken W. & Seilacher A. (Eds.): Cycles and events in stratigraphy. *Springer-Verlag*, Berlin–Heidelberg, 377–382.

Einsele G., Ricken W. & Seilacher A. (Eds.) 1991a: Cycles and events in stratigraphy. *Springer-Verlag*, Berlin–Heidelberg, 1–955.

Einsele G., Ricken W. & Seilacher A. 1991b: Cycles and events in stratigraphy — Basic concepts and terms. In: Einsele G., Ricken W. & Seilacher A. (Eds.): Cycles and events in stratigraphy. *Springer-Verlag*, Berlin–Heidelberg, 1–19.

Fernández-López S.R. 2007: Ammonoid taphonomy, palaeoenvironments and sequence stratigraphy at the Bajocian/Bathonian boundary on the Bas Auran area (Subalpine Vasin, south-eastern France). *Lethaia* 40, 377–391.

Fernández-López S. & Fernández-Jalvo Y. 2002: The limit between biostratinomy and fossildiagenesis. In: De Renzi M., Pardo Alonso M.V., Belinchón M., Peñalver E., Montoya P. &. Márquez-Aliaga A. (Eds.): Current topics on taphonomy and fossilization. *Int. Conference Taphos 2002*, Valencia, 27–36.

Fernández-López S.R., Henriques M.H. & Duarte L.V. 2002: Taphonomy of Ammonite Condensed Associations — Jurassic examples from Carbonate Platforms of Iberia. *Abh. Geol. Bundesanst.* 57, 423–430.

Flügel E. 1978: Mikrofazielle Untersuchungsmethoden von Kalken. *Springer-Verlag*, Berlin–Heidelberg–New York, 1–454.

Flügel E. 2004: Microfacies of carbonate rocks. Analysis, interpretation and application. *Springer-Verlag,* Berlin–Heidelberg, 1–976.

Futterer E. 1982: Experiments on the distinction of wave and current influenced shell accumulation. In: Einsele G. & Seilacher A. (Eds.): Cyclic and event and stratification. *Springer-Verlag*, Berlin–Heidelberg, 175–179.

Fürsich F.T. & Pandey D.K. 1999: Genesis and environmental significance of Upper Cretaceous shell concentrations from the Cauvery Basin, southern India. *Palaeogeogr. Palaeoclimatol. Palaeoecol.* 145, 119–139.

Gallet Y., Krystyn L., Marcoux J. & Besse J. 2007: New constraints on the end-Triassic (Upper Norian–Rhaetian) magnetostratigraphy. *Earth Planet. Sci. Lett.* 255, 458–470.

Gindl A. 2000: Paläoökologie triassischer Ammonitenfaunen des Taurusgebirges (Türkei). *Unpubl. Diploma Thesis*, *Univ. Vienna*, 1–80.

Goldring R. 1991: Fossils in the field. Information potential and analysis. *Longman Scientific & Technical*, 1–218.

Golebiowski R. 1991: Becken und Riffe der alpinen Obetrias. Lithostratigraphie und Biofazies der Kössener Formation. In: Nagel D. & Rabeder G. (Eds.): Exkursionen im Jungpaläozoikum und Mesozoikum Österreichs. *Österr. Paläont. Gesell.*, Wien, 79–119.

Golonka J. 2004: Plate tectonic evolution of the southern margin of Eurasia in the Mesozoic and Cenozoic. *Tectonophysics* 381, 235–273.

Göncüoğlu C.M., Sayit K. & Tekin U.K. 2010: Oceanization of the northern Neotethys: geochemical evidence from ophiolitic melange basalts within the İzmir-Ankara suture belt, NW Turkey. *Lithos* 116, 175–187.

Gradstein F.M., Ogg J.G., Schmitz M.D. & Ogg G.M. 2012: The Geologic Time Scale 2012. Volume 2. *Elsevier*, Boston, 437–1144.

Gutnic M., Monod O., Poisson A. & Dumont J.F. 1979: Géologie des Taurides Occidentales (Turquie). *Mém. Soc. Géol. France* 137, 1–112.

Hips K. 1998: Lower Triassic storm-dominated ramp sequence in northern Hungary: an example of evolution from homoclinal through distally steepened ramp to Middle Triassic flat-topped platform. In: Wright V.P. & Burchette T.P. (Eds.): Carbonate ramps. *Geol. Soc. London, Spec. Publ.* 149, 315–338.

Hladil J., Čejchan P., Gabašová A., Táborský Z. & Hladíková J. 1996: Sedimentology and orientation of tentaculite shells in turbidite lime mudstone to packstone: Lower Devonian, Barrandian, Bohemia. *J. Sed. Res.* 66, 888–899.

Hoedemaeker P.J. 1994: Ammonite distribution around the Hauterivian-Barremian boundary along the Río Argos (Caravaca, SE Spain). *Géol. Alpine* 20, 219–277.

Hornung T. 2008: The Carnian crisis in the Tethys Realm. *Verlag Dr. Müller*, Saarbrücken, 1–235.

Howell D.G. & Normark W.R. 1982: Sedimentology of submarine fans. In: Scholle P.A. & Spearing D. (Eds.): Sandstone depositional environments. *Amer. Assoc. Petrol. Geol., Mem.* 31, 365–404.

Kawakami G. & Kawamura M. 2002: Sediment flow and deformation (SFD) layers: evidence for intrastratal flow in laminated muddy sediments of the Triassic Osawa Formation, northeast Japan. *J. Sed. Res.* 72, 171–181.

Kemper E., Rawson P.F. & Thieuloy J.P. 1981: Ammonites of Tethyan ancestry in the early lower Cretaceous of northwest Europe. *Palaeontology* 24, 2, 251–311.

Kidwell S.M. 1986: Models for fossil concentrations: paleobiologic implications. *Palebiology* 12, 6–24.

Kidwell S.M. 1988: Taphonomic comparison of passive and active continental margins: Neogene shell beds of the Atlantic coastal plain and northern Gulf of California. *Palaeogeog. Palaeoclimatol. Palaeoecol.* 63, 201–224.

Kidwell S.M. 1991a: The stratigraphy of shell concentrations. In: Allison P.A. & Briggs D.E.G. (Eds.): Taphonomy: Releasing the data locked in the fossil record. Topics in geobiology. Volume 9. *Plenum Press*, New York, 211–290.

Kidwell S.M. 1991b: Taphonomic feedback (Live/dead intercations) in the genesis of bioclastic beds: Keys to reconstruction sedimentary dynamics. In: Einsele G., Ricken W. & Seilacher A. (Eds.): Cycles and events in stratigraphy. *Springer-Verlag*, Berlin–Heidelberg, 268–282.

Kidwell S.M. 1993a: Patterns of time-averaging in shallow marine fossil assemblages. In: Kidwell S.M. & Behrensmeyer A.K. (Eds.): Taphonomic approaches to time resolution in fossil assemblage. *Paleont. Soc. Shortcourse* 6, 275–300.

Kidwell S.M. 1993b: Taphonomic expressions of sedimentary hiatus: field observations on bioclastic concentrations and sequence anatomy in low, moderate and high subsidence settings. *Geol. Rdsch.* 82, 189–202.

Kidwell S.M. & Bosence D.W.J. 1991: Taphonomy and time-averaging of marine shelly faunas. In: Allison P.A. & Briggs D.E.G. (Eds.): Taphonomy: Releasing the data locked in the fossil record. Topics in geobiology. Volume 9. *Plenum Press*, New York, 115–209.

Kidwell S.M., Fürsich F.T. & Aigner T. 1986: Conceptual framework for the analysis and classification of fossil concentrations. *Palaios* 1, 228–238.

Kreisa R.D. & Bambach R.K. 1982: The role of storm processes in generating shell beds in Palaeozoic shelf environments. In: Einsele G. & Seilacher A. (Eds.): Cyclic and event and stratification. *Springer-Verlag*, Berlin–Heidelberg, 200–207.

Krystyn L., Gallet Y., Besse J. & Marcoux J. 2002: Integrated Upper Carnian to Lower Norian biochronology and implications for the Upper Triassic magnetic polarity time scale. *Earth. Planet. Sci. Lett.* 203, 343–351.

Lowe D.R. 1982: Sediment gravity flows. II. Depositional models with special reference to the deposits of high-density turbidity currents. *J. Sed. Petrology* 52, 279–297.

Lukeneder A. 2001: Palaeoecological and palaeooceanographical significance of two ammonite mass-occurrences in the Alpine Lower Cretaceous. *PhD. Thesis, Univ. Vienna*, 1–316.

Lukeneder A. 2003a: The *Karsteniceras* Level: Dysoxic ammonoid beds within the Early Cretaceous (Barremian, Northern Calcareous Alps, Austria). *Facies* 49, 87–100.

Lukeneder A. 2003b: Ammonoid stratigraphy of Lower Cretaceous successions within the Vienna Woods (Kaltenleutgeben section, Lunz Nappe, Northern Calcareous Alps, Lower Austria). In: Piller W.E. (Ed.): Stratigraphia Austriaca. *Österr. Akad. Wiss., Schr. d. Erdwiss. Komm.* 16, 165–191.

Lukeneder A. 2004a: Late Valanginian ammonoids: Mediterranean and Boreal elements — implications on sea-level controlled migration (Ebenforst Syncline; Northern Calcareous Alps; Upper Austria). *Aust. J. Earth Sci.* 95, 96, 46–59.

Lukeneder A. 2004b: The *Olcostephanus* Level: An Upper Valanginian ammonoid mass-occurrence (Lower Cretaceous, Northern Calcareous Alps, Austria). *Acta Geol. Pol.* 54, 1, 23–33.

Lukeneder A. (in print) 2014: Ammonoid habitats and life history. In: Klug C. & Korn D. (Eds.): Cephalopods present and past. 9. Ammonoid paleobiology. *Springer*, Dordrecht.

Lukeneder S. & Lukeneder A. 2014: A new Ammonoid Fauna from the Carnian (Upper Triassic) Kasımlar Formation of the Taurus Mountains (Anatolia, Turkey). *Palaeontology* 57, 2, 357–396. Open Access. Doi: 10.1111/pala.12070

Lukeneder S., Lukeneder A. & Weber G.W. 2014: Computed reconstruction of spatial ammonoid-shell orientation captured from digitized grinding and landmark data. *Computers & Geosciences* 64, 104–114.

Lukeneder S., Lukeneder A., Harzhauser M., Islamoglu Y., Krystyn L. & Lein R. 2012: A delayed carbonate factory breakdown during the Tethyan-wide Carnian pluvial episode along the Cimmerian terranes (Taurus, Turkey). *Facies* 58, 279–296.

Maeda H. 1999: Did ammonoid carcasses surface or sink? *Mem. Geol. Soc. Japan* 54, 131–140.

Maeda H. & Seilacher A. 1996: Ammonoid taphonomy. In: Landman N.H., Tanabe K. & Davis R.A. (Eds.): Ammonoid paleobiology. Vol. 13. Topics in Geobiology. *Plenum Press*, New York, 543–578.

Maeda H. & Shigeta Y. 2009: Ammonoid mode of occurrence. In: Shigeta Y., Zakharov Y.D., Maeda H. & Popov A.M. (Eds.): The Lower Triassic system in the Abrek Bay area, South Primorye, Russia. *Nat. Mus. Nat. Sci., Monographs* 38, 36–38.

Manfrin S., Mietto P. & Preto N. 2005: Ammonoid biostratigraphy of the Middle Triassic Latemar platform (Dolomites, Italy) and its correlation with Nevada and Canada. *Geobios* 38, 477–504.

Martin R.E. 1999: Taphonomy. A process approach. In: Briggs D.E.G., Dodson P., MacFadden B.J., Sepkoski J.J. & Spicer R.A. (Eds.): Cambridge paleobiology. Series 4. *Cambridge University Press*, 1–508.

Mayrhofer S. & Lukeneder A. (in prep): Taphonomy and palaeoecology of Carnian (Upper Triassic) ammonoid shell beds from the Taurus Mountain, South Turkey. Fossil ammonoid mass occurrence (*Kasimlarceltites krystyni*) as key to a Carnian environment (Taurus Mountains, Turkey). *Lethaia*.

McRoberts C.A. 2010: Biochronology of Triassic bivalves. In: Lucas S.G. (Ed.): The Triassic timescale. *Geol. Soc. London, Spec. Publ.* 334, 201–219.

Meldahl K.H. 1993: Geographic gradients in the formation of shell concentration: Plio-Pleistocene marine deposits, Gulf of California. *Palaeogeogr. Palaeoclimatol. Palaeoecol.* 101, 1–25.

Middleton G.V. & Hampton M.A. 1973: Sediment gravity flows: mechanics of flow and deposition. In: Middleton G.V. & Bouma A.H. (Eds.): Turbitites and deep water sedimentation. Short course notes. *Soc. Econ. Paleont. Mineralogists, Spec. Publ.*, Anaheim, 1–23.

Middleton G.V. & Hampton M.A. 1976: Subaqueous sediment transport and deposition by sediment gravity flows. In: Stanley D.J. & Swift D.J.P. (Eds.): Marine sediment transport and environmental management. *Wiley*, New York, 197–218.

Monod O. 1977: Recherches géologiques dans le Taurus Occidental

au sud de Beyşehir (Turquie). *PhD. Thesis*, *Univ. South Paris*, 1–442.

Montiel-Boehringer A.Y., Ledesma-Vásquez J. & Avila-Serrano G.E. 2011: Fossil beds, gravity flows, and sand waves during the Pliocene: Gulf of California. *J. Coast. Res.* 27, 549–554.

Mulder T. & Alexander J. 2001: The physical character of subaqueous sedimentary density flows and their deposits. *Sedimentology* 48, 269–299.

Murphy M.A. & Salvador A. (Eds.) 1999: International stratigraphic guide — An abridged version. *Episodes* 22, 4, 255–271.

Müller A.H. 1963: Lehrbuch der Paläozoologie. 1. Allgemeine Grundlagen. C. Die Fossilisationslehre. *Fischer*, Jena, 17–134.

Nichols G. 2009: Sedimentology and stratigraphy. *Wiley-Blackwell*, Pondicherry, 419.

Niechwedowicz M. & Trammer J. 2007: Hydrodynamically controlled anagenetic evolution of Famenian goniatites from Poland. *Acta Palaeont. Pol.* 52, 63–75.

Noe-Nygaard N., Surlyk F. & Piasecki S. 1987: Bivalve mass mortality caused by toxic dinoflagellate blooms in a Berriasian–Valanginian lagoon, Bornholm, Denmark. *Palaios* 2, 263–273.

Norris R.D. 1986: Taphonomic gradients in shelf fossil assemblages: Pliocene Purisma Formation, California. *Palaios* 1, 256–270.

Olivero E.B. 2007: Taphonomy of ammonites from the Santonian–Lower Campanian Santa Marta Formation, Antarctica: Sedimentological controls on vertically embedded ammonites. *Palaios* 22, 586–597.

Olóriz F. 2000: Time averaging and long term palaeoecology in macroinvertebrate fossil assemblages with ammonites (Upper Jurassic). *Rev. Paléobiol., Spec. Vol.* 8, 123–140.

Olóriz F. & Villaseñor A.B. 2010: Ammonite biogeography: From descriptive to dynamic, ecological interpretations. In: Tanabe K., Shigeta Y., Sasaki T. & Hirano H. (Eds.): Cephalopods — Present and past. *Tokai University Press*, Tokyo, 253–265.

Özgül N. & Arpat E. 1973: Structural units of Taurus orogenic belt and their continuation in the neighbouring regions. *Geol. Soc. Greece Bull.* 10, 156–164.

Pérez-Lopéz A. & Pérez-Valera F. 2012: Tempestite facies models for the epicontinental Triassic carbonates of the Betic Cordillera (southern Spain). *Sedimentology* 59, 646–678.

Poisson A. 1977: Recherches géologiques dans les Taurides occidentals (Turquie). *PhD. Thesis*, *Univ. South Paris*, 1–759.

Potter P.E. & Pettijohn F.J. 1977: Paleocurrents and basin analysis. 2nd corrected and updated edition. *Springer–Verlag*, Berlin–Göttingen–Heidelberg, 1–425.

Potter P.E., Maynard J.B. & Depetris P.J. 2005: Mud & mudstones. *Springer*, Berlin–Heidelberg, 1–297.

Radley J.D. & Barker M.J. 1998: Palaeoenvironmental analysis of shell beds in the Waelden Group (Lower Cretaceous) of the Isle of Wight, southern England: an initial account. *Cretaceous Research* 19, 489–504.

Robertson A.H.F. 1993: Mesozoic-Tertiary sedimentary and tectonic evolution of Neotethyan carbonate platforms, margins and small ocean basins in the Antalya Complex, southwest Turkey. *Int. Assoc. Sed., Spec. Publ.* 20, 415–465.

Robertson A.H.F. 2000: Mesozoic-Tertiary tectonic-sedimentary evolution of a south Tethyan Oceanic Basin and its margins in southern Turkey. *Geol. Soc. London, Spec. Publ.* 173, 97–138.

Robertson A.H.F., Poisson A. & Akıncı Ö. 2003: Developments in research concerning Mesozoic-Tertiary Tethys and neotectonics in the Isparta Angle, SW Turkey. *Geol. J.* 38, 195–234.

Salvador A. 1994: International stratigraphic guide (A guide to stratigraphic classification, terminology and procedure). 2nd Ed., XIX + 214 Intern. *Union Geol. Sci.* and *Geol. Soc. Amer.*, 1–214.

Scotese C.R. 1998: Quicktime computer animations. PALEOMAP Project, Department of Geology. *University of Texas at Arlington*, Arlington.

Scotese C.R. 2001: Paleomap Project. http://www.scotese.com/ (July 2001).

Scotese C.R., Gahagan L.M. & Larson R.L. 1989: Plate tectonic reconstructions of the Cretaceous and Cenozoic ocean basins. In: Scotese C.R. & Sager W.W. (Eds.): Mesozoic and Cenozoic plate reconstructions. *Elsevier*, Amsterdam, 27–48.

Seilacher A. 1968: Sedimentationsprozesse in Ammoniten-Gehäusen. *Akad. Wiss. Lit., Abh. Math.-Naturwiss. Kl.* 9, 191–203.

Seilacher A. & Aigner T. 1991: Storm deposition at the bed, facies, and basin scale: the geological perspective. In: Einsele G., Ricken W. & Seilacher A. (Eds.): Cycles and events in stratigraphy. *Springer-Verlag*, Berlin–Heidelberg, 249–267.

Sepkoski J.J. Jr., Bambach R.K. & Droser M.L. 1991: Secular changes Phanerozoic event bedding and the biological overprint. In: Einsele G., Ricken W. & Seilacher A. (Eds.): Cycles and events in stratigraphy. *Springer-Verlag*, Berlin–Heidelberg, 298–312.

SEPM Strata (2014): Deepwater processes & sediment. SEPM stratigraphy. Web — http://sepmstrata.org (accessed 11 January 2014).

Soja C.M., Gobetz K.E., Thibeau J., Zavala E. & White B. 1996: Taphonomy and paleobiological implications of Middle Devonian (Eifelian) nautiloid concentrations, Alaska. *Palaios* 11, 422–436.

Speyer S.E. & Brett C.E. 1991: Taphofacies controls. Backround and episodic processes in fossil asseblage preservation. In: Allison P.A. & Briggs D.E.G. (Eds): Taphonomy. Releasing the data locked in the fossil record. Topics in geobiology. 9. *Plenum Press*, New York & London, 501–545.

Stampfli G.M. & Borel G.D. 2002: A plate tectonic model for the Paleozoic and Mesozoic constrained by dynamic plate boundaries and restored synthetic oceanic isochrons. *Earth Planet. Sci. Lett.* 196, 17–33.

Stampfli G.M., Borel G.D., Marchant R. & Mosar J. 2002: Western Alps geological constraints on western Tethyan reconstructions. *J. Virtual. Explor.* 8, 77–106.

Steininger F.F. & Piller W.E. 1999: Empfehlungen (Richtlinien) zur Handhabung der stratigraphischen Nomenklatur. *Cour. Forsch.-Inst. Senckenberg* 209, 1–19.

Storms J.E.A. 2001: Simulating event deposition: effects of storms on the shallow marine stratigraphic record. *IAMG extended abstract*, September 2001, Cancun, 1–19.

Stow D.A.V. & Mayall M. 2000: Deep-water sedimentary systems: New models for the 21st century. *Mar. Petrol. Geol.* 17, 125–135.

Şenel M. 1997: 1:250,000 scaled Turkey Geological map, Isparta section. 4. [Türkiye Jeoloji Haritalari. Nr. 4. Isparta Paftasi.] *Mineral Research and Exploration General Directorate, Geological Department*, Ankara, 1–47 (in Turkish).

Şengör A.M.C. & Yılmaz Y. 1981: Tethyan evolution of Turkey: A plate tectonic approach. *Tectonophysics* 75, 181–241.

Şengör A.M.C., Yılmaz Y. & Sungurlu O. 1984: Tectonics of the Mediterranean Cimmerids: Nature and evolution of the western termination of Paleo-Tethys. *Geol. Soc. London, Spec. Publ.* 17, 77–112.

Tekin U.K. & Göncüoğlu C. 2007: Discovery of the oldest (Upper Ladinian to Middle Carnian) radiolarian assemblages from the Bornova Flysch zone in Western Turkey: implications for the evolution of the Neotethyan İzmir–Ankara Ocean. *Ofioliti* 32, 131–150.

Tekin U.K., Göncüoğlu C. & Turhan N. 2002: First evidence of Late Carnian radiolarians from the İzmir–Ankara suture complex, central Sakarya, Turkey: implications for the opening age of the İzmir–Ankara branch of Neo-Tethys. *Geobios* 35, 127–135.

Tucker M.E. & Wright V.P. 1990: Carbonate sedimentology. *Blackwell Scientific Publications*, Oxford, London, Edinburgh, 1–482.

Westermann G.E.G. 1996: Ammonoid life and habitat. In: Landman N.H., Tanabe K. & Davis R.A. (Eds.): Ammonoid paleobiology. Topics in geobiology. Vol. 13. *Plenum Press*, New York 857, 607–707.